# BCAP functions as a dynamic regulator of hematopoiesis and myeloid cell development

Jeffrey Mitchell Duggan

A dissertation

submitted in partial fulfillment of the

requirements for the degree of

Doctor of Philosophy

University of Washington

2017

Reading Committee:

Jessica A. Hamerman, Chair

Daniel B. Stetson

Kevin B. Urdahl

Program Authorized to Offer Degree:

Department of Immunology

University of Washington

## Abstract

BCAP functions as a dynamic regulator of hematopoiesis and myeloid cell development

Jeffrey Mitchell Duggan

Chair of the Supervisory Committee:
Affiliate Associate Professor Jessica A. Hamerman
Department of Immunology

Hematopoiesis governs the production of mature cells of the lymphoid, myeloid and erythroid lineages. This process occurs in the bone marrow of adult mammals, and generates these lineages throughout life. Furthermore, hematopoiesis is sensitive to multiple insults that drive demand for new hematopoietic cell differentiation, including infection, inflammation and myeloablation. These situations of demand alter hematopoietic differentiation to favor myeloid cell production, in a process known as emergency myelopoiesis. Both steady state hematopoiesis and emergency myelopoiesis are tightly regulated by a variety of signals in order to properly control the output of the different hematopoietic lineages. BCAP (B cell adaptor for PI-3 kinase) is a signaling adaptor protein expressed in hematopoietic cells, where it has a wide array of functions. Here we show that BCAP is expressed in the Hematopoietic Stem and

Progenitor cells in the bone marrow, and acts as an inhibitor of myeloid cell development in both the steady state and during demand situations. Furthermore, we show that BCAP inhibits proliferation of the Long-Term Hematopoietic Stem cells, and therefore may regulate the quiescence and/or the self-renewal of this population in the BM. Overall, we have identified BCAP as a novel dynamic regulator of hematopoiesis and myeloid cell development.

# TABLE OF CONTENTS

# LIST OF TABLES

# LIST OF FIGURES

# ACKNOWLEDGEMENTS

First and foremost, the author would like to thank Dr. Jessica Hamerman, who has been an amazing mentor and for her insights, patience and wisdom throughout graduate school. The author would also like to acknowledge the all the people who assisted this work. These include Dr. Matthew Buechler, Rebecca Olson, and Dr. Tobias Hohl, who all contributed to the work published in Blood. Furthermore, this work could not have been completed without the assistance of all members of the Hamerman lab, who have been incredibly helpful in all facets of my scientific and personal life. The author would also like to acknowledge Dr. Kevin Urdahl, Dr. Daniel Stetson, and Dr. David Rawlings for serving on my dissertation committee and for providing useful insight to my projects over the last 4 years. The author would also like to acknowledge Dr. Daniel Campbell, Dr. Steven Ziegler, Dr. Estelle Bettelli, and Dr. Adam Lacy-Hulbert, as well as the personnel in their labs for their assistance and support regarding this work. Furthermore, the author would like to acknowledge the personnel at the Benaroya Research Institute and UW Immunology, including program coordinators Peggy McCune and Sandy Turner, for their assistance and contributions to my graduate education. An immense thank you to all of you.

# DEDICATION

This dissertation has been completed in memory of my paternal grandparents, John and Patricia Duggan, and my maternal grandfather, George Kemp, whom all held hard work and good education in the highest regard.

For my grandmother, Clara Kemp, who achieved her bachelor's degree at the age of 58, and has always supported me throughout my life and heavily encouraged applying oneself to their education.

For my parents, George and Donna Duggan, and my brother, Andrew Duggan, for their unwavering support and love, especially as I moved so far away from home for graduate school.

For Frank and Nancy Eidson, the parents of my fiancée Kelly, who have been heroes of mine throughout graduate school and for their gracious support.

For the love of my life, Kelly Eidson, who has stood by me through these many years of graduate school and always made sure I believed in myself. Thank you, my love, forever and always.

# CHAPTER 1: INTRODUCTION

Hematopoiesis governs the production of mature cells of the erythroid, lymphoid and myeloid lineages[1,2]. These hematopoietic cells provide critical functions to vertebrate biology, including oxygen transport, blood clotting, host defense and immunity. Hematopoiesis begins in bone marrow (BM) in adult mammals, including mice, with the quiescent, self-renewing Long-Term Hematopoietic Stem Cells (LT-HSC), that provides life-long generation of mature hematopoietic cells (Figure 1.1). LT-HSC differentiate into Short-Term (ST) HSC, and subsequently into Multipotent Progenitors (MPP), which have decreased self-renewal capacity and differentiate into all the hematopoietic lineages. In mice, the LT-HSC, ST-HSC and MPP populations together are identified by their absence of mature Lineage markers, and their expression of CD117 (cKit) and Sca-1, and are therefore called $Lin^{-}Sca1^{+}cKit^{+}$ (LSK) cells. The MPP differentiate into lineage-specific progenitors that produce lymphoid cells, the Common Lymphoid Progenitor (CLP), and myeloid cells, the Common Myeloid Progenitor (CMP). The CMP then differentiates into more committed progenitors, including the Megakaryocyte-Erythrocyte Progenitor (MEP), the Common Dendritic Progenitor (CDP), and the Granulocyte-Macrophage Progenitor (GMP), and produce mature cells of erythroid, dendritic cell, and granulocyte-macrophage lineages, respectively[3,4]. Together, these populations are collectively called the Hematopoietic Stem and Progenitor cells (HSPC).

Hematopoiesis is tightly regulated to ensure continual replacement of these mature hematopoietic lineages in the steady state. During demand situations, including myeloablation and infection, hematopoiesis is altered to favor myeloid cell generation at the expense of lymphoid generation, known as emergency myelopoiesis[5]. Emergency myelopoiesis is induced

by a variety of cytokines and other danger signals, which act directly on HSPC. These include agonists for several Toll-like receptors (TLR), including TLR2[6], TLR4[6,7], and TLR7[8], and cytokines including G-CSF[9,10], IL-3[11], IL-6[12-14], IFNγ[15], and Type I Interferons[16,17]. Altogether, a wide variety of cytokines, transcription factors and signaling pathways control hematopoiesis at both the steady-state and during demand situations.

Multiple factors govern myelopoiesis, including transcription factors and growth factors. The transcription factor Pu.1 is the master regulator of myelopoiesis, and governs differentiation of LSK into CMP and CLP, and its deletion results in a lack of all myeloid cells and B cells in adult mice[18,19]. The transcription factor C/EBPα regulates CMP differentiation into GMP and supports granulocyte differentiation[20], whereas the transcription factor IRF8 cooperates with Pu.1 to promote monocyte differentiation from GMP[21]. A number of cytokines modulate myelopoiesis both at the steady state and during infection. The cytokines of the Colony-Stimulating Factor family (CSF), including Granulocyte-CSF (G-CSF), Macrophage-CSF (M-CSF) and Granulocyte/Macrophage-CSF (GM-CSF) have been well characterized as stimulators of myelopoiesis and each instruct HSPC to differentiate into distinct lineages[22,23]. G-CSF promotes neutrophil differentiation, and G-CSF$^{-/-}$ mice have severe reductions in circulating neutrophil numbers[9]. M-CSF, which signals through CSF1R (CD115), is critical for monocyte development, as M-CSF$^{-/-}$ mice are devoid of monocytes[24,25], and can instruct myeloid differentiation within HSC[26]. GM-CSF can stimulate the differentiation of both neutrophils and monocytes[27], and is critical for maintaining myeloid development during infection[28]. However, GM-CSF$^{-/-}$ mice exhibit normal hematopoiesis, but are lacking in certain tissue macrophage populations, including alveolar macrophages[27,29]. Overall, these factors and others govern the production of myeloid cells both at the steady state and during situations of demand.

The LT-HSC represent the least-differentiated population among hematopoietic cells, and produce all the hematopoietic lineages throughout life[30]. Hematopoiesis drives differentiation of LT-HSC to ST-HSC, and subsequently to MPP cells, which lose their self-renewal capacity, are highly proliferative, and differentiate into lineage-restricted progenitor cells. The LT-HSC pool must balance the ability to remain quiescent with the capacity to self-renew, and with their potential to proliferate and differentiate into the hematopoietic progenitors that produce the mature hematopoietic lineages. The control of these states is critical for both the production of new erythroid, lymphoid and myeloid cells throughout life, while also adapting to rapidly respond to hematopoietic needs during demand situations, including infection or myeloablation[5].

Multiple factors control the maintenance of the LT-HSC population in the BM, including transcription factors, cell cycle regulators and cytokines and chemokines. Proliferation in LT-HSC is coupled with their differentiation into MPP cells, and therefore causes them to leave their quiescent state and lose their capacity to self-renew[31]. The transcription factors Scl, Runx1 and GATA2 all maintain the balance between HSC quiescence and self-renewal[32], often working within the same transcriptional network[33]. Scl is highly expressed in LT-HSC and maintains their numbers through inhibiting cell cycle progression[34]. Runx1 is required for the emergence of LT-HSC during embryonic development[1]. GATA2 is also critical for LT-HSC formation during development, and promotes the survival of LT-HSC during adult hematopoiesis[35,36]. Furthermore, LT-HSC quiescence in the in $G_0$ stage of the cell cycle is controlled by multiple cell cycle regulators, including p21, p53, and CDK6[31,33]. The cytokine Stem Cell Factor (SCF), which signals through the receptor cKit (CD117), promotes the survival and self-renewal of LT-HSC[31]. The chemokine CXCL12 (SDF-1), which binds to CXCR4, retains LT-HSC within the BM and maintains HSC quiescence[33]. These factors, as well as others, ensure the maintenance

of the LT-HSC in the BM, and therefore the steady production of hematopoietic cells, throughout life,

B-cell adaptor for PI3-kinase (BCAP) is a signaling adaptor protein expressed in cells of the hematopoietic lineage (Figure 1.2)[37]. BCAP was first identified in B cells, where it activates Phosphoinositol-3 kinase (PI3K) downstream of the B-cell receptor (BCR)[38]. Upon BCR ligation, BCAP becomes phosphorylated at its four YxxM motifs and binds to the p85 subunit of PI3K, therefore mediating PI3K activation. BCAP is a positive regulator of B cell development and homeostasis, and BCAP$^{-/-}$ mice have reduced mature B cell numbers[37,39]. BCAP is recruited to the BCR through interactions with the adaptor protein Nck[40]. BCAP promotes PI3K activation in conjunction with CD19[41], which is critical for B cell development in the BM[42]. Accordingly, BCAP$^{-/-}$ mice had fewer pre-B cells in the BM, and decreased numbers of B1 cells and mature B cells in the spleen compared to WT mice[37]. Furthermore, BCAP has been shown to mediate NFκB activation in mature B cells, as c-Rel expression was decreased in BCAP$^{-/-}$ B cells, resulting in reduced B cell proliferation and survival after BCR stimulation in the absence of BCAP[39]. BCAP is also expressed in Natural Killer (NK) cells, where it functions as a negative regulator of NK cell maturation and function, as BCAP$^{-/-}$ NK cells survive longer and have more functional activity compared to WT NK cells[43]. More recently, we and others showed that BCAP functions in macrophages to promote PI3K activation downstream of Toll-like Receptor (TLR) ligation, thereby negatively regulating TLR-induced inflammation[44,45]. These findings demonstrated that BCAP is expressed in both myeloid and lymphoid lineages, and can perform varying functions within different hematopoietic cell populations.

As a signaling adaptor protein, BCAP contains several protein-protein interaction domains in addition to YxxM tyrosines important for PI3K binding (Figure 1.2). These include

ankyrin repeats, a DBB domain, coiled-coil domains, proline-rich sequences and a "cryptic-TIR domain[37,38,45]." This multi-domain structure suggests BCAP may interact with many signaling pathways. In fact, proteomic analysis of BCAP-interacting proteins in bone narrow-derived macrophages has identified a variety of binding partners for BCAP, suggesting broad functions in these cells (Ni, James and Hamerman, unpublished observations). This suggests that BCAP can interact with several other signaling pathways outside of PI3K activation, and thus may have multiple unique functions in hematopoietic cells.

Here we show that BCAP is expressed in the HSPC in the bone marrow, and acts as an inhibitor of myeloid cell development in both the steady state and during demand situations. Furthermore, we show that BCAP maintains LT-HSC numbers and inhibits LT-HSC proliferation at the steady state, suggesting that BCAP is critical for HSC quiescence and/or self-renewal. Overall, we have identified BCAP as a novel dynamic regulator of hematopoiesis and myeloid cell development.

**Chapter 1 Figures**

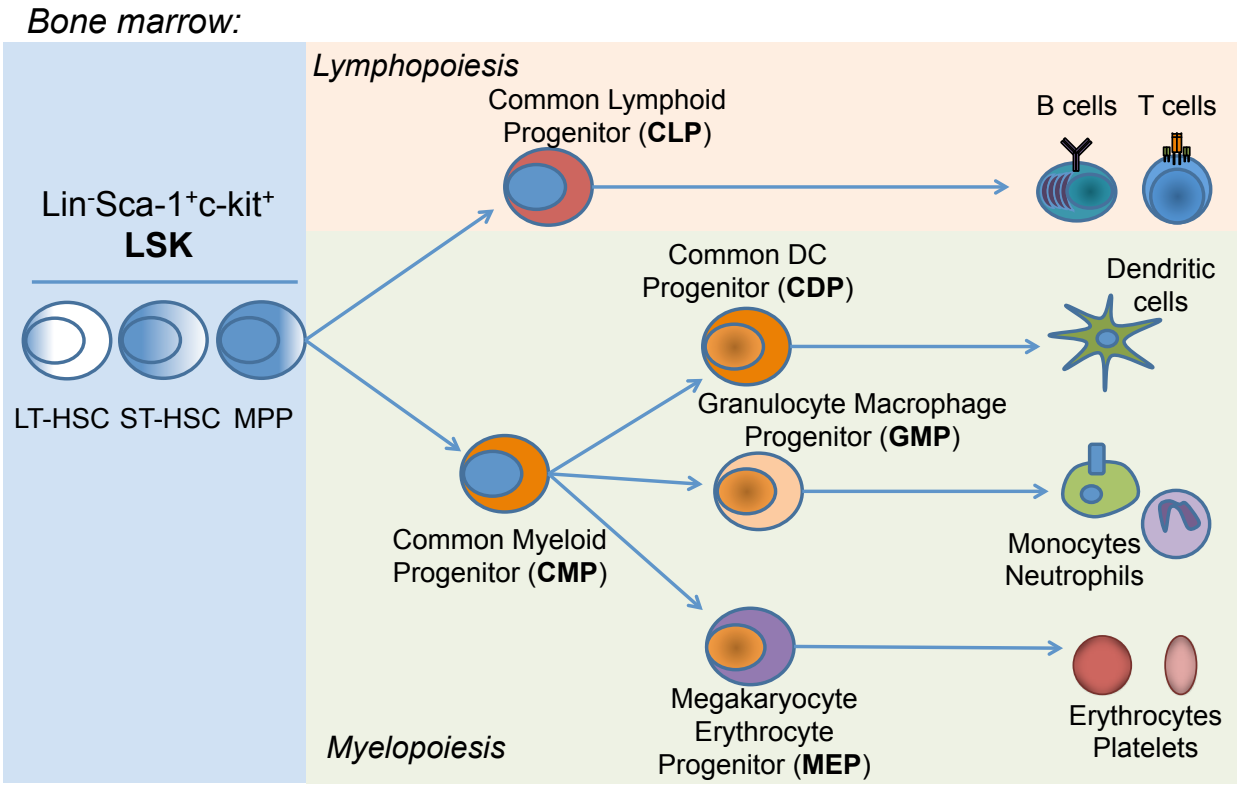


**Figure 1.1. Diagram of hematopoiesis.** Diagram of hematopoietic differentiation as it occurs within the bone marrow of mice. Blue shaded box shows the LSK compartment (containing the Hematopoietic Stem cells and Multipotent Progenitors). Tan shaded box shows lymphopoiesis. Green shaded box shows myelopoiesis.

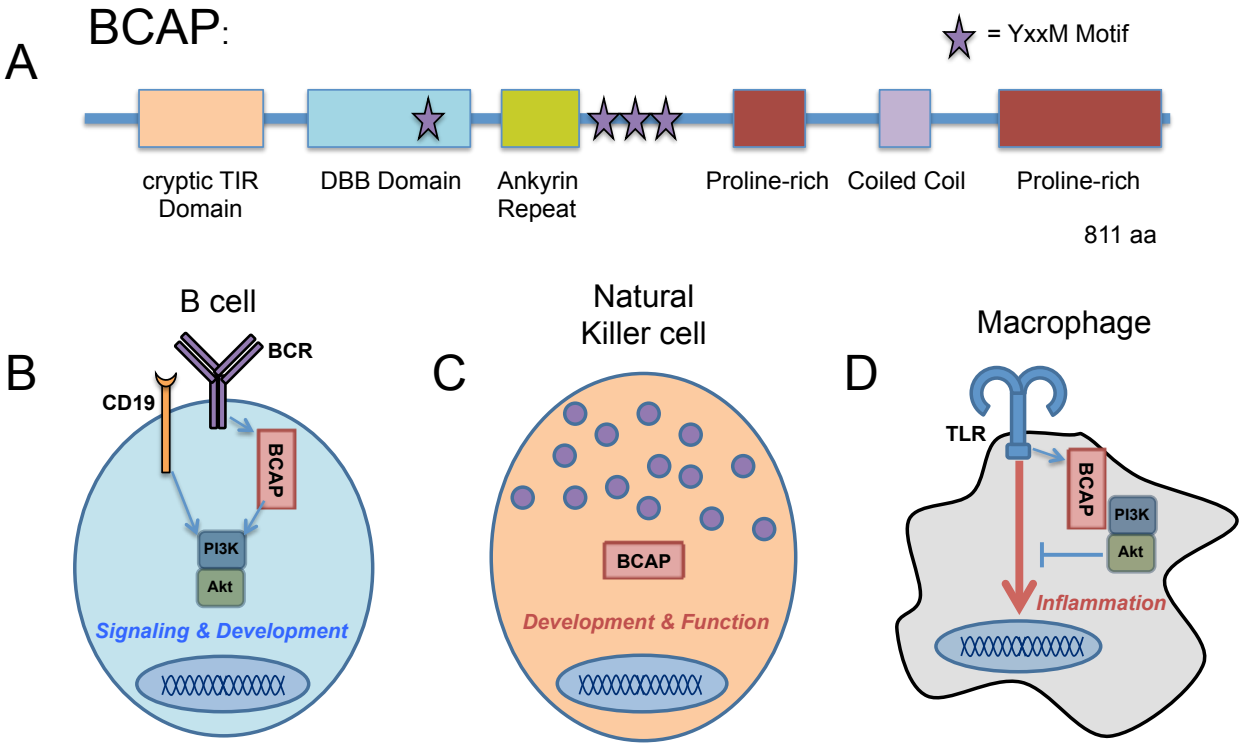


**Figure 1.2. Diagrams of protein domains within BCAP and identified functions for BCAP.** (A) Schematic of the protein domains present within BCAP (with YxxM motifs marked as indicated) throughout its 811 amino acid-long structure. (B) Schematic of the positive regulatory role of BCAP in B cell receptor (BCR) signaling and B cell development. (C) Schematic of the negative regulatory role of BCAP in Natural Killer (NK) cell development and function. (D) Schematic of the negative regulatory role of BCAP in TLR signaling in macrophages. Positive and negative regulatory roles are written in *blue* and *red* italics, respectively (B-D).

# CHAPTER 2: BCAP INHIBITS PROLIFERATION AND DIFFERENTIATION OF MYELOID PROGENITORS IN THE STEADY STATE AND DURING DEMAND SITUATIONS

**Abstract**

B cell adaptor for PI3-kinase (BCAP) is a signaling adaptor expressed in mature hematopoietic cells including monocytes and neutrophils. Here we investigated the role of BCAP in the homeostasis and development of these myeloid lineages. BCAP$^{-/-}$ mice had more bone marrow (BM) monocytes than WT mice, and in mixed WT:BCAP$^{-/-}$ BM chimeras, monocytes and neutrophils skewed towards BCAP$^{-/-}$ origin, showing a competitive advantage for BCAP$^{-/-}$ myeloid cells. BCAP was expressed in bone marrow hematopoietic progenitors, including LSK (Lineage$^{-}$Sca1$^{+}$cKit$^{+}$), CMP (Common Myeloid Progenitor) and GMP (Granulocyte/Macrophage Progenitor) cells. At the steady state, BCAP$^{-/-}$ GMP expressed more IRF8 and less CEBPα than WT GMP, which correlated with an increase in monocyte progenitors and a decrease in granulocyte progenitors amongst GMP. Strikingly, BCAP$^{-/-}$ progenitors proliferated and produced more myeloid cells of both neutrophil and monocyte/macrophage lineages than WT progenitors in myeloid colony forming unit (CFU) assays, supporting a cell-intrinsic role of BCAP in inhibiting myeloid proliferation and differentiation. Consistent with these findings, during cyclophosphamide-induced myeloablation or specific monocyte depletion, BCAP$^{-/-}$ mice replenished circulating monocytes and neutrophils earlier than WT mice. During myeloid replenishment after cyclophosphamide-induced myeloablation, BCAP$^{-/-}$ mice had increased LSK proliferation, and increased numbers of LSK and GMP cells, compared to WT mice. Furthermore, BCAP$^{-/-}$ mice accumulated more monocytes and neutrophils in the spleen than WT

mice during *Listeria monocytogenes* infection. Together, these data identify BCAP as a novel inhibitor of myelopoiesis in the steady state and of emergency myelopoiesis during demand conditions.

**Introduction**

Hematopoiesis governs the production of mature cells of the erythroid, lymphoid and myeloid lineages[1]. Hematopoiesis begins in bone marrow (BM) in adult mice, with the quiescent, self-renewing Long-Term Hematopoietic Stem Cells (LT-HSC), that provides life-long generation of mature hematopoietic cells. Hematopoiesis from LT-HSC occurs through a series of progenitor cells that have increasingly restricted lineage potential throughout their differentiation[3,4]. Hematopoiesis ensures maintenance of all lineages in the steady-state. However, this process is tightly regulated to respond to demand situations, including myeloablation and infection, when hematopoiesis is accelerated and altered to favor myeloid cell generation at the expense of lymphoid cell generation, known as emergency myelopoiesis[5]. A wide variety of signaling pathways and transcription factors regulate hematopoiesis at both the steady-state and during demand situations allowing for control of this dynamic system.

B cell adaptor for PI3-kinase (BCAP) is a signaling adaptor protein expressed in hematopoietic cells[37]. BCAP was identified in B cells, where it activates PI3K downstream of the B cell receptor[38], and is a positive regulator of B cell development and homeostasis[37,39]. BCAP is also expressed in Natural Killer cells, where it functions as a negative regulator of maturation and function[43]. More recently, we and others showed that in mature macrophages BCAP promotes PI3K activation downstream of Toll-like Receptors (TLR), thereby negatively regulating TLR-induced inflammation[44,45]. Thus, BCAP is expressed in both myeloid and lymphoid lineages and can perform varying functions within different hematopoietic cell populations. Here we show that BCAP is expressed within hematopoietic stem and progenitor cells (HSPC) and functions as a novel negative regulator of myeloid cell development.

## Materials and Methods

### Mice, BM chimeras and in vivo treatments

All mice were bred at the Benaroya Research Institute, and C57BL/6 and B6.SJL mice were also purchased from Jackson Laboratories. BCAP$^{-/-}$ mice[37] with a disrupted *Pik3ap1* gene were back-crossed nine generations to C57BL/6 background, and Ccr2-depleter mice[46] were bred to C57BL/6 or BCAP$^{-/-}$ mice. All experiments were performed under an IACUC-approved protocol.

Mixed BM chimeras were generated by lethally irradiating (1000 rad) recipient C57BL/6 x B6.SJL F1 mice and reconstituting with a 1:1 ratio of $5x10^6$ B6.SJL (CD45.1$^+$) and either $5x10^6$ C57BL/6 (CD45.2$^+$) or BCAP$^{-/-}$ (CD45.2$^+$) BM cells. For experiments with Ccr2-depleter mice, mice were injected i.p. with 10 ng/g Diphtheria Toxin (DT) (List Biological Laboratories) in PBS. For myeloablation experiments, mice were injected i.p. with 175 mg/kg cyclophosphamide (Sigma-Aldrich) in PBS. For proliferation, mice were injected i.p. with 1 mg/mL BrdU for 1 hour. BrdU incorporation was assayed using the BD BrdU Flow Kit (BD Biosciences). Blood samples were obtained via saphenous vein. For infection experiments, mice were injected i.v. with 3000 CFU of *L. monocytogenes* strain 10403S.

### Cell isolation and staining

Mouse splenocytes, blood cells, and BM cells were isolated and stained with antibodies for flow cytometry as previously described[17,47]. Lineage$^-$ BM cells were isolated using a Lineage Cell Depletion Kit (Miltenyi Biotec). Intracellular staining for BCAP was conducted by fixing lineage$^-$ BM cells with Cytofix/Cytoperm buffer and staining in Perm/Wash buffer (BD Biosciences). Cells were blocked with rat IgG (Sigma-Aldrich), stained with mouse anti-BCAP IgG1 antibody, and then stained anti-mouse IgG1-Allophycocyanin (BD Biosciences), followed

by staining for surface proteins with all steps conducted at 4°C. Apoptosis was analyzed by staining for Annexin-V with Annexin-V Binding Buffer (eBioscience) and Propidium Iodide (Sigma-Aldrich). Intranuclear staining for IRF8 was conducted by fixing and permeabilizing sorted lineage$^-$ BM cells with FoxP3/Transcription Factor Fixation/Permeabilization buffer (Tonbo). Intracellular staining for TNF and iNOS was conducted by incubating cells for 4 hours at 37°C in GolgiPlug (BD Biosciences) directly ex vivo, followed by permeabilization and intracellular staining. All mAbs used for flow cytometry are listed in Table 2.1. Data were acquired using an LSR II or FACSCanto (BD Biosciences) and analyzed using FlowJo software (TreeStar). Doublets were excluded from live cell gating using forward light scatter and side scatter. Cell sorting was conducted using a FACSAria II (BD Biosciences). Cells were quantified by flow cytometry using polystyrene counting beads (Polysciences).

**In vitro progenitor differentiation and BrdU incorporation**

Progenitor CFU assays were conducted using Methocult GF M3534 (containing SCF, IL-3 and IL-6) or M3234 (StemCell Technologies) with 50 ng/mL M-CSF (Gibco), 50 ng/mL GM-CSF or 50 ng/mL G-CSF (PeproTech) as previously described[17]. For BrdU incorporation, cells were removed from Methocult and incubated in StemPro-34 SFM Complete media (Thermo Fisher) containing 10 μg/mL BrdU for 1-4 hours at 37°C. For CMP to GMP differentiation, 5000 cells were sorted into StemPro-34 SFM Complete media with 50 ng/mL SCF (Thermo Fisher), 10 ng/mL IL-3 (PeproTech), and IL-6 (BioLegend), and incubated at 37°C for up to 24 hours. Cells were stained with anti-CD16/32 mAb, fixed, and analyzed by flow cytometry.

**Quantitative Real-Time PCR**

Samples were prepared as previously described[17,47] and SYBR-green-based quantitative RT-PCR was performed on a ABI 7500Fast Real-Time PCR system. Primer sequences are listed in Table 2.2.

**Statistical analyses**

Data were analyzed by Student's unpaired *t* test using Prism (GraphPad).

## Results

### BCAP differentially regulates myeloid and lymphoid cell development and/or homeostasis

The role of BCAP in the development and homeostasis of myeloid cells has not been investigated. We therefore examined the numbers of neutrophils and monocytes of WT and BCAP$^{-/-}$ mice in the steady-state. WT and BCAP$^{-/-}$ mice had similar numbers of CD11b$^{+}$Ly6G$^{+}$Ly6C$^{int}$ neutrophils in the BM, blood and spleen, and similar numbers of CD115$^{+}$CD11b$^{+}$Ly6G$^{-}$Ly6C$^{-}$ resident monocytes in the blood (Figure 2.1). However, whereas WT and BCAP$^{-/-}$ mice had similar numbers of CD11b$^{+}$Ly6G$^{-}$Ly6C$^{hi}$ inflammatory monocytes in the blood and spleen, BCAP$^{-/-}$ BM had a significant ~25% increase in inflammatory monocyte numbers compared to WT BM. Increases in the percentage of neutrophils and inflammatory monocytes in the spleen were likely due to the decrease in mature B cells (not shown)[37,39].

To determine whether this increased monocyte number in BCAP$^{-/-}$ BM was cell-intrinsic, we created mixed BM chimeras by transferring congenically marked WT (CD45.1$^{+}$) and BCAP$^{-/-}$ (CD45.2$^{+}$) BM at a 1:1 ratio to lethally irradiated F1 recipient mice (CD45.1$^{+}$CD45.2$^{+}$) followed by reconstitution for >8 weeks. Whereas WT:WT chimeras reconstituted inflammatory monocytes in a ~1:1 ratio, BCAP$^{-/-}$:WT chimeras exhibited a ~2.5:1 ratio of BCAP$^{-/-}$ into WT monocytes in the BM, blood, and spleen (Figure 2.2A-B). This selective advantage for BCAP$^{-/-}$ cells was also present within neutrophils (Figure 2.2A-B). In contrast, splenic follicular and marginal zone B cells were skewed towards WT origin, showing a selective disadvantage for BCAP$^{-/-}$-derived B cells (Figure 2.2C). Therefore, BCAP plays distinct roles in myeloid and lymphoid cell development and/or homeostasis.

We asked whether the competitive advantage of BCAP$^{-/-}$ myeloid cells may be due to increased survival compared to their WT counterparts, and therefore we examined ex vivo

apoptosis by staining monocytes and neutrophils for Annexin-V and Propidium Iodide. However, we found that WT and BCAP$^{-/-}$ neutrophils and monocytes undergo apoptosis at similar rates (Figure 2.3). Because this selective advantage of BCAP$^{-/-}$ myeloid cells began in the BM and was independent of cell survival, we hypothesized that BCAP regulates myeloid cell development within the BM.

**BCAP is expressed within hematopoietic stem and progenitor cells**

Inflammatory monocytes and neutrophils develop during myelopoiesis from HSPC in the BM[4]. To determine if BCAP regulates myelopoiesis, we first examined whether BCAP is expressed within BM HSPC. BCAP was expressed in Lineage$^{-}$Sca-1$^{+}$c-kit$^{+}$ (LSK), Common Myeloid Progenitor (CMP), and Granulocyte-Macrophage Progenitor (GMP) populations, whereas no BCAP expression was detected in Megakaryocyte-Erythrocyte Progenitor (MEP) cells (Figure 2.4A-B, Figure 2.5A-B). LSK cells expressed the highest amount of BCAP, whereas BCAP expression was similar in CMP and GMP cells. We also examined BCAP expression in the LT-HSC, Short-term HSC (ST-HSC) and Multipotent Progenitor (MPP) populations using CD150 and CD48 to identify these cells amongst LSK (Figure 2.4A). BCAP was expressed as early as LT-HSC, and had the highest expression in MPP cells (Figure 2.5C-D). Therefore, BCAP is expressed at the earliest stages of hematopoiesis and exhibits sustained expression throughout myelopoiesis, suggesting that BCAP may play a role in this process.

**BCAP$^{-/-}$ mice have similar numbers of hematopoietic progenitors to WT mice**

Because in the steady-state BCAP$^{-/-}$ BM had an increased number of inflammatory monocytes and a competitive advantage in repopulating myeloid lineages, we hypothesized that

BCAP$^{-/-}$ mice may have increased BM progenitor populations. Contrary to our hypothesis, we found similar numbers and frequencies of LSK, CMP, GMP and MEP cells within WT and BCAP$^{-/-}$ BM (Figure 2.4Bm Figure 2.6A). WT and BCAP$^{-/-}$ mice also had similar numbers of Common Lymphoid Progenitors (CLP) within the BM (Figure 2.4C-D). Therefore BCAP$^{-/-}$ mice exhibit similar progenitor homeostasis as WT mice in the steady state.

**Altered myeloid-specifying transcription factor expression in BCAP$^{-/-}$ progenitors**

Although WT and BCAP$^{-/-}$ mice have similar numbers of myeloid progenitors, we hypothesized that BCAP may affect the expression of transcription factors that control myelopoiesis[48]. Pu.1, the master regulator of myeloid differentiation, governs the differentiation of LSK into CMP and CLP[18,19]. C/EBPα regulates CMP differentiation into GMP and supports granulocyte differentiation[20], whereas IRF8 cooperates with Pu.1 to promote monocyte differentiation from GMP[21].

We examined the expression of Pu.1, C/EBPα and IRF8 by qRT-PCR in sorted progenitors. Pu.1 was expressed at similar or slightly increased levels in WT and BCAP$^{-/-}$ LSK, CMP and GMP cells (Figure 2.6B). BCAP$^{-/-}$ LSK and CMP had significantly increased expression of C/EBPα and IRF8 compared to WT cells, whereas BCAP$^{-/-}$ GMP had less C/EBPα and higher IRF8 than WT GMP. When examining IRF8 protein levels in progenitors, we found that BCAP$^{-/-}$ mice had a greater proportion of IRF8$^{+}$ LSK, CMP and GMP (Figure 2.6C-D). However, the amount of IRF8 protein per cell, as measured by MFI of the IRF8-expressing population, was similar in WT and BCAP$^{-/-}$ progenitor cells. Therefore, the increased number of IRF8$^{+}$ progenitors combined with the decreased expression of C/EBPα in BCAP$^{-/-}$ GMP suggests that BCAP$^{-/-}$ GMP may favor monocyte over granulocyte production in the steady state,

consistent with the increased monocyte numbers found in the BM of BCAP$^{-/-}$ mice (Figure 2.1B).

**Increased proportion of monocyte progenitors in BCAP$^{-/-}$ mice**

Recently, several subsets of GMPs were identified through differential expression of Ly6C and CD115[49]. Ly6C$^{lo}$CD115$^{lo}$ oligopotent GMP (Early GMP) differentiated into both monocytes and neutrophils. Ly6C$^{hi}$CD115$^{lo}$ GMP differentiated primarily into neutrophils and were termed Granulocyte Progenitors (GP), whereas Ly6C$^{hi}$CD115$^{hi}$ GMP primarily differentiated into monocytes and were called Monocyte Progenitors (MP). Due to the increased frequency of IRF8$^{+}$ cells and decreased expression of C/EBPα in BCAP$^{-/-}$ GMP, we examined whether BCAP$^{-/-}$ GMP have altered frequencies of MP and GP compared to WT GMP. Indeed, BCAP$^{-/-}$ mice had an increased frequency of MP and a decreased frequency of GP than WT mice, whereas the frequency of Early GMP was similar (Figure 2.6E-F). Therefore, while progenitor frequencies are identical between WT and BCAP$^{-/-}$ mice up to the Early GMP stage, BCAP$^{-/-}$ mice have more MP, suggesting steady state myelopoiesis in BCAP$^{-/-}$ mice may favor monocyte differentiation over neutrophil differentiation.

**BCAP$^{-/-}$ myeloid progenitors out-compete WT progenitors in mixed BM chimeras**

Next, we asked whether BCAP$^{-/-}$ progenitors have a competitive advantage compared to WT progenitors by examining their repopulation in mixed BM chimeras reconstituted with equal numbers of WT and BCAP$^{-/-}$ BM. In these mixed chimeras, CMP cells were significantly skewed towards BCAP$^{-/-}$ origin, and LSK, GMP and MEP cells had a trend in skewing towards BCAP$^{-/-}$ origin (Figure 2.4E). In contrast, CLP populations in BCAP$^{-/-}$: WT chimeras were

similar to WT:WT control chimeras (Figure 2.4F). Therefore, BCAP deficiency may confer a selective advantage for myeloid and megakaryocyte-erythroid progenitors, but does not appear to affect lymphoid progenitors.

**Increased myeloid cell production from BCAP$^{-/-}$ HSPC**

To directly assess whether BCAP-deficient HSPC have an increased capacity to produce myeloid cells, we sorted LSK, CMP and GMP cells into methylcellulose media containing SCF, IL-3 and IL-6, which drives granulocyte and macrophage colony differentiation. At day 5, WT and BCAP$^{-/-}$ LSK, CMP and GMP formed similar numbers of total colonies and of Granulocyte, Macrophage, and mixed Granulocyte/Macrophage colonies (Figure 2.7A). However, when we quantified the cell yields in the cultures, BCAP$^{-/-}$ LSK, CMP and GMP produced significantly more cells than their WT counterparts (Figure 2.7B). Interestingly, BCAP$^{-/-}$ GMP cultures produced increased numbers of both mature macrophages and neutrophils compared to WT GMP cultures (Figure 2.7C, Figure 2.8A), suggesting that upon strong cytokine stimulation, BCAP$^{-/-}$ progenitors lose their bias towards monocyte production and produce more cells of both the monocyte/macrophage and neutrophil lineages.

To determine if this increased cell yield is unique to specific myelopoiesis-promoting cytokines, we sorted WT and BCAP$^{-/-}$ GMP into methylcellulose media containing M-CSF, GM-CSF, or G-CSF. Similarly to the SCF, IL-3, and IL-6 cultures, BCAP$^{-/-}$ GMP produced more myeloid cells than their WT counterparts in response to M-CSF and GM-CSF, while minimal differences were apparent in G-CSF-stimulated cultures (Figure 2.8B). Additionally, BCAP$^{-/-}$ cultures stimulated with GM-CSF produced more mature macrophages and neutrophils than WT

cultures (Figure 2.7D). Thus, similar to the skewing in mixed BM chimeras, BCAP$^{-/-}$ progenitors cell-intrinsically produce increased numbers of myeloid cells compared to WT progenitors.

Because BCAP$^{-/-}$ HSPC produced more myeloid cells, we hypothesized that BCAP limits either survival or proliferation during myeloid differentiation. BCAP$^{-/-}$ LSK cultures had more, not less, active Caspase-3$^{+}$ cells than WT at day 6 post-culture (Figure 2.8C), showing that the increased cell yield was not due to BCAP$^{-/-}$ cells being more resistant to apoptosis. We next examined proliferation in the methylcellulose cultures using BrdU incorporation. At all days of culture examined, BCAP$^{-/-}$ LSK-derived cells incorporated more BrdU than their WT counterparts (Figure 2.7E). Similarly, at day 4, BCAP$^{-/-}$ CMP-derived cells incorporated more BrdU than their WT counterparts. GMP cultures had very low BrdU incorporation and we found no significant difference in WT and BCAP$^{-/-}$ GMP cultures at any times examined. Thus, cultures derived from early BCAP$^{-/-}$ progenitors have increased proliferation and produce more myeloid cells than those from WT progenitors, supporting a model in which BCAP restrains myeloid differentiation via suppressing progenitor proliferation in a cell-intrinsic manner.

Due to the increase in cells produced by BCAP$^{-/-}$ HSPC, we asked whether BCAP regulates the maturation of myeloid progenitors. As shown previously, the differentiation of CMP into GMP cells can be observed ex vivo by up-regulation of the Fcγ receptors CD16/32. BCAP$^{-/-}$ CMP cultures had more CD16/32$^{hi}$ cells than WT cultures starting at 4 hours, with this increase being maintained throughout the culture (Figure 2.9A-B). Therefore, BCAP$^{-/-}$ CMP exhibited accelerated differentiation into GMP compared to WT CMP.

**BCAP$^{-/-}$ have an increased proportion of IL-6Rα$^{+}$ cells among HSPC**

Because BCAP$^{-/-}$ mice had an increased proportion of IRF8$^{+}$ cells in all HSPC (Figure 2.6D), we next asked if BCAP$^{-/-}$ HSPC are better primed for myeloid differentiation. Myelopoiesis is predominantly induced by cytokine signals, including by IL-6[50,51]. The IL-6 receptor is comprised of the IL-6 receptor alpha subunit (IL-6Rα) and the gp130 chain, both of which are expressed on HSPC[13,52]. Because the IL-6/IL-6Rα axis promotes myelopoiesis during infection and myeloablation[12,14,52-54], we examined the expression of the IL6Rα subunit on WT and BCAP$^{-/-}$ HSPC. As expected, IL-6Rα was expressed at increasing levels on HSPC as monocyte/neutrophil commitment increased, from LSK to CMP to GMP (Figure 2.10A). Interestingly, BCAP$^{-/-}$ LSK, CMP, and GMP had significantly more IL-6Rα$^{hi}$ cells than their WT counterparts (Figure 2.10B), suggesting that BCAP regulates HSPC fate decision from as early as the LSK stage to inhibit myeloid cell production.

**BCAP$^{-/-}$ mice have increased monocytes and neutrophils during demand situations**

During situations of demand, such as infection or myeloablation, hematopoiesis adapts to produce increased numbers of myeloid cells in a process known as emergency myelopoiesis. To determine if BCAP controls monocyte and neutrophil production during demand situations, we used several in vivo models. First, we utilized Ccr2-depleter mice, in which the gene for the simian Diphtheria Toxin (DT) receptor is expressed under control of the regulatory elements for *Ccr2*[46], which is highly expressed in inflammatory monocytes[55]. A single dose of DT in Ccr2-depleter mice depletes mature inflammatory monocytes for 48 hours. After a single DT injection, we compared the reconstitution of blood inflammatory monocytes and neutrophils in WT/Ccr2-depleter and BCAP$^{-/-}$/Ccr2-depleter mice. Monocytes were similarly depleted from WT/Ccr2-depleter and BCAP$^{-/-}$/Ccr2-depleter mice by 24 hours post-DT treatment, and depletion

was maintained for 48 hours (Figure 2.11A). At 96 hours post-DT treatment, BCAP$^{-/-}$/Ccr2-depleter mice had fully replenished their circulating monocytes to steady-state numbers, whereas WT/Ccr2-depleter mice had replenished their monocytes to only ~50%. BCAP$^{-/-}$/Ccr2-depleter mice also had increased numbers of neutrophils in the blood compared to WT/Ccr2-depleter mice, suggesting that replenishment of monocytes occurs from a bi-potent progenitor with monocyte and neutrophil potential. Therefore, after specific monocyte depletion, BCAP$^{-/-}$ monocytes are replenished faster than WT monocytes, with a concomitant increase in circulating neutrophil numbers.

We also examined monocyte and neutrophil replenishment after myeloablation with the chemotherapeutic cyclophosphamide. Cyclophosphamide causes rapid depletion of mature myeloid cells followed by recovery due to new hematopoiesis[56,57]. A single dose of cyclophosphamide induced monocyte and neutrophil depletion to ~1% of pretreatment numbers in both WT and BCAP$^{-/-}$ mice by 48 hours (Figure 2.11B). Strikingly, BCAP$^{-/-}$ mice had fully replenished their circulating monocytes and neutrophils to steady-state levels by 96 and 120 hours, respectively, while WT mice had only reached ~40% of steady-state levels at these time points. Therefore, BCAP$^{-/-}$ mice replenish their monocytes and neutrophils faster than WT mice after cyclophosphamide-induced myeloablation.

Due to this accelerated replenishment of mature myeloid cells in BCAP$^{-/-}$ mice, we hypothesized that BCAP$^{-/-}$ HSPC cells would have increased proliferation after cyclophosphamide treatment compared to WT mice. BCAP$^{-/-}$ LSK cells exhibited increased BrdU incorporation in comparison to WT LSK cells 48 hours after cyclophosphamide treatment (Figure 2.11C-D), while BrdU incorporation was not significantly different in WT and BCAP$^{-/-}$ CMP and GMP cells. Furthermore, BCAP$^{-/-}$ mice exhibited increased numbers of LSK and

GMP cells compared to WT mice by 48 hours post-cyclophosphamide (Figure 2.11E). Therefore, the increase in monocyte and neutrophil reconstitution after cyclophosphamide treatment correlated with changes in HSPC.

Lastly, we examined monocyte and neutrophil numbers during infection with the Gram-positive bacteria *Listeria monocytogenes* (*Lm*). Neutrophils and $CCR2^{+}$ monocytes accumulate in the spleen during *Lm* infection and monocytes are critical for *Lm* clearance[55,58-60]. Concurrently, this infection-induced demand drives emergency myelopoiesis in the BM for rapid production of monocytes and neutrophils to further combat *Lm*[61,62]. In WT mice, monocyte numbers rose in the spleen at day 2 after *Lm* infection, and peaked at day 3 post-infection (Figure 2.11F). In contrast, $BCAP^{-/-}$ mice reached peak monocyte numbers in the spleen at day 2 post-infection, a full day ahead of WT mice. Neutrophil numbers peaked at day 2 post-infection for both WT and $BCAP^{-/-}$ mice, however peak neutrophil numbers were significantly higher in $BCAP^{-/-}$ mice. Consistent with the critical role monocytes play during *Lm* infection[55,58,59], $BCAP^{-/-}$ mice had increased numbers of activated monocytes, as determined by TNF and iNOS staining, in the spleen at day 2 post-infection compared to WT mice, despite a lower frequency of $TNF^{+}$ and $iNOS^{+}$ monocytes in the spleen of $BCAP^{-/-}$ mice compared to WT mice at this time point (Figure 2.12). Furthermore, the increased accumulation of monocytes and neutrophils $BCAP^{-/-}$ mice correlates with increased clearance of *Lm* in the spleen and liver compared to WT mice (Figure 2.11G). Therefore, in demand situations requiring rapid emergency myelopoiesis, BCAP serves to restrain monocyte and neutrophil generation.

**Discussion**

Here, we show that BCAP$^{-/-}$ mice exhibit an increased ability to generate myeloid cells from their HSPC compared to WT mice. Specifically, BCAP$^{-/-}$ HSPC produced more myeloid cells than WT HSPC both in culture, and in vivo at the steady state and during demand situations (Figure 2.13). Whereas BCAP has several different functions in mature hematopoietic cells, we have identified a unique role for BCAP during myelopoiesis.

The most profound effect of BCAP during myelopoiesis is its ability to restrain differentiation and proliferation of HSPC when they are placed in demand situations. In the CFU assays, where HSPC are removed from their niche and induced to proliferate and differentiate with strong cytokine signals, BCAP$^{-/-}$ LSK, CMP and GMP all produced increased numbers of myeloid cells compared to WT cells. In all three in vivo situations of demand-adapted myelopoiesis we examined, including cell ablation and bacterial infection, BCAP$^{-/-}$ mice also showed an increased output of monocytes and neutrophils at early times. Furthermore, in the Ccr2-depleter model, though only inflammatory monocytes were specifically depleted, both monocyte and neutrophil numbers were increased in BCAP$^{-/-}$ mice, showing the effect of BCAP is on an oligopotent progenitor, not a committed monocyte progenitor, in this model. That BCAP can inhibit demand-adapted myelopoiesis in these diverse models suggests that BCAP regulates a critical early step in these processes.

Proliferation of HSPC is modulated by multiple factors, including cytokines, signaling pathways and transcription factors[5,6,48,63,64]. BCAP$^{-/-}$ HSPC exhibited increased proliferation both in the CFU assays, as well as during cyclophosphamide-induced myeloablation. Interestingly, BCAP$^{-/-}$ GMP produced increased numbers of myeloid cells than WT GMP in response to M-CSF, GM-CSF, and combined SCF, IL-3 and IL-6, cytokines that signal in from

distinct receptors, suggesting that BCAP regulates expression or function of a downstream common component of diverse signaling pathways.

In addition to restraining proliferation, BCAP may also contribute to increased demand-adapted myelopoiesis by slowing differentiation. Indeed, we found that BCAP-deficient CMP progressed to the GMP stage faster than WT GMP, and BCAP-deficient GMP generated mature macrophages in response to GM-CSF faster than WT cells. Similarly, during infection with *Listeria monocytogenes*, BCAP-deficient mice generated myeloid cells faster than WT mice by day 2 after infection. Whereas many studies have investigated factors that regulate HSPC proliferation, little is known about what regulates the speed of this process and how this links to proliferation, which increases as HSPC become more committed. Our study shows BCAP is a novel inhibitor of this process.

We also found that in the absence of BCAP, all HSPC populations examined had increased proportions of IL-6Rα$^{+}$ cells. IL-6R signaling on HSPC blocks lymphopoiesis and increases myelopoiesis[13,53]. As IL-6 is induced during infection[14,65], autoimmunity[13], and cyclophosphamide-induced myeloablation[57,66], IL-6 signaling likely is critical for altering hematopoiesis during demand situations and the increased frequency of IL-6Rα$^{+}$ cells we see in BCAP$^{-/-}$ HSPC may contribute to increased emergency myelopoiesis in BCAP$^{-/-}$ mice. We also identified IL-6Rα expression as a marker of HSPC maturation along the myeloid differentiation pathway, and therefore the increased proportion of IL-6Rα$^{hi}$ cells among BCAP$^{-/-}$ HSPC suggests they are more myeloid-primed than WT HSPC.

In addition to its potent effects on HSPC proliferation in demand situations, in the steady state, BCAP affects the GMP stage of myelopoiesis. BCAP$^{-/-}$ GMP cells appear more primed for monocyte differentiation, as their GMP cells are enriched for IRF8$^{+}$ cells and Ly6C$^{hi}$CD115$^{hi}$

MP cells[49,67]. This correlates with BCAP$^{-/-}$ mice having increased BM monocyte numbers at the steady-state. Interestingly, we see increases in both monocytes and neutrophils in the demand-adapted situations we examined, suggesting that during emergency myelopoiesis new monocyte and neutrophil production originates from earlier HSPC populations such as LSK or CMP cells.

BCAP was originally described to activate PI3K by interacting with the p85 subunit of PI3K upon phosphorylation of its four YxxM motifs[37,38]. However, BCAP contains several protein-protein interaction domains, including ankyrin repeats, a DBB domain, coiled-coil domains, proline-rich sequences and a "cryptic-TIR domain[37,45]." Thus BCAP may interact with several signaling pathways in addition to PI3K. Preliminary studies examining signaling pathways within BCAP$^{-/-}$ HSPC suggests that BCAP does not impact PI3K signaling during progenitor CFU assays, as phosphorylation of the PI3K/mTOR target ribosomal protein S6 was not decreased in BCAP$^{-/-}$ progenitor-derived cells (J.M. Duggan and J.A. Hamerman, unpublished observations). Additionally, lower PI3K activation, as would be predicted in BCAP$^{-/-}$ HSPC, would be expected to reduce, not promote, myeloid differentiation, given the positive role of PI3K in myelopoiesis[8,68]. We have also not found a direct effect of BCAP in regulating proximal STAT3 activation downstream of IL-6 (J.M. Duggan and J.A. Hamerman, unpublished observations), an important cytokine in our in vitro CFU assays and in emergency myelopoiesis in vivo[13,14,57,65,66]. Therefore, identifying the signaling pathways BCAP regulates to inhibit myeloid differentiation is of particular interest. Overall, we have identified BCAP as a novel negative regulator of myeloid cell development from hematopoietic progenitors. Defining novel regulators of emergency myelopoiesis is important to understanding this critical process, and for future efforts to therapeutically accelerate monocyte and neutrophil reconstitution following myeloablation after BM transplantation or chemotherapy.

## Chapter 2 Tables

| Antibody | Clone | Conjugate | Source | Dilution |
|---|---|---|---|---|
| Ly6C | HK1.4 | FITC | BioLegend | 1:400 |
| Ly6G | 1A8 | Pacific Blue | BioLegend | 1:200 |
| CD11b | M1/70 | PerCP-Cy5.5; Biotin | eBioscience | 1:600 |
| CCR2 | 475301 | APC | R&D Systems | 10 µL/ test |
| CD115 | AFS98 | APC; PE | eBioscience | 1:100 |
| CD45.1 | A20 | BV421; PE-Cy7 | BioLegend | 1:100 |
| CD45.2 | 104 | APC; Af700 | eBioscience | 1:100 |
| CD19 | eBio1D3; 6D5 | Af700; APC; Biotin | eBioscience; BioLegend | 1:100 |
| CD45R (B220) | RA3-6B8 | PerCP-Cy5.5; APC-ef780 | eBioscience | 1:100 |
| TCRβ | H57-597 | APC-ef780 | eBioscience | 1:200 |
| CD21 | 7G6 | PE | BD Biosciences | 1:500 |
| CD23 | B3B4 | PE-Cy7 | eBioscience | 1:250 |
| F4/80 | BM8 | Biotin | eBioscience | 1:100 |
| Gr1 | RB6-8C5 | Biotin | eBioscience | 1:600 |
| CD11c | N418 | Biotin | eBioscience | 1:100 |
| CD3 | eBio500a2 | Biotin | eBioscience | 1:100 |
| NK1.1 | PK136 | Biotin | eBioscience | 1:100 |
| CD127 (IL-7Rα) | A7R34 | Pacific Blue; BV605; Biotin | BioLegend; eBioscience | 1:100 |
| Streptavidin | ---------- | APC-ef780 | eBioscience | 1:100 |
| CD34 | RAM34 | FITC; Af700 | eBioscience | 1:10 |
| Sca-1 | D7 | PerCP-Cy5.5; BV510 | eBioscience | 1:100 |
| CD117 | 2B8 | PE-Cy7 | eBioscience | 1:100 |
| CD16/32 | 93 | PE; Pacific Blue | BioLegend | 1:100 |
| CD48 | HM48-1 | PerCP-Cy5.5; PE | BioLegend | 1:100 |
| CD150 | RC15-12F12.2 | Pacific Blue | BioLegend | 1:100 |
| BCAP (mouse IgG1) | 4L8E6 | ---------- | Ref. 8 | 1:16000 |
| α-mouse IgG1 | A85-1 | APC | BD Biosciences | 1:100 |
| CD126 (IL-6Rα) | D7715A7 | PE | BioLegend | 1:100 |
| α-BrdU | MoBU-1 | Pacific Blue | Invitrogen | 5 µL/ test |
| IRF8 | V3GYWCH | APC | eBioscience | 1:100 |
| Rat IgG1 κ Isotype | eBRG1 | APC | eBioscience | 1:100 |
| iNOS | Rabbit polyclonal | ---------- | Millipore | 1:50 |
| α-rabbit IgG | Goat $F(ab')_2$ polyclonal | PE | Jackson Laboratories | 1:1000 |
| TNF | MP6-XT22 | PE | eBioscience | 1:100 |
| F4/80 | BM8 | BV421 | BioLegend | 1:200 |
| Annexin-V | purified protein | APC | eBioscience | 5 µL/ test |
| Propidium Iodide | ---------- | ---------- | Sigma-Aldrich | 5 µL/ test |

**Table 2.1: Antibodies used for flow cytometry and cell sorting**

| Gene | Primer sequences | Source |
|---|---|---|
| HPRT | F 5'- TGAAGAGCTACTGTAATGATCAGTCAAC -3'<br>R 5'- AGCAAGCTTGCAACCTTAACCA -3' | IDT |
| Pu.1 | F 5'- AGGCGTGCAAAATGGAAGGG -3'<br>R 5'- GTGCGGAGAAATCCCAGTAGT -3' | IDT |
| C/EBPα | F 5'- GCGGGAACTCAACAACATC -3'<br>R 5'- GTCACTGGTCAACTCCAGCAC -3' | IDT |
| IRF8 | F 5'- GACCATGTTTATCCCCTGGAA -3'<br>R 5'- GGGACCGGTCAGTCACTTCTTCA -3' | IDT |

**Table 2.2: Primers used for qRT-PCR**

## Chapter 2 Figures

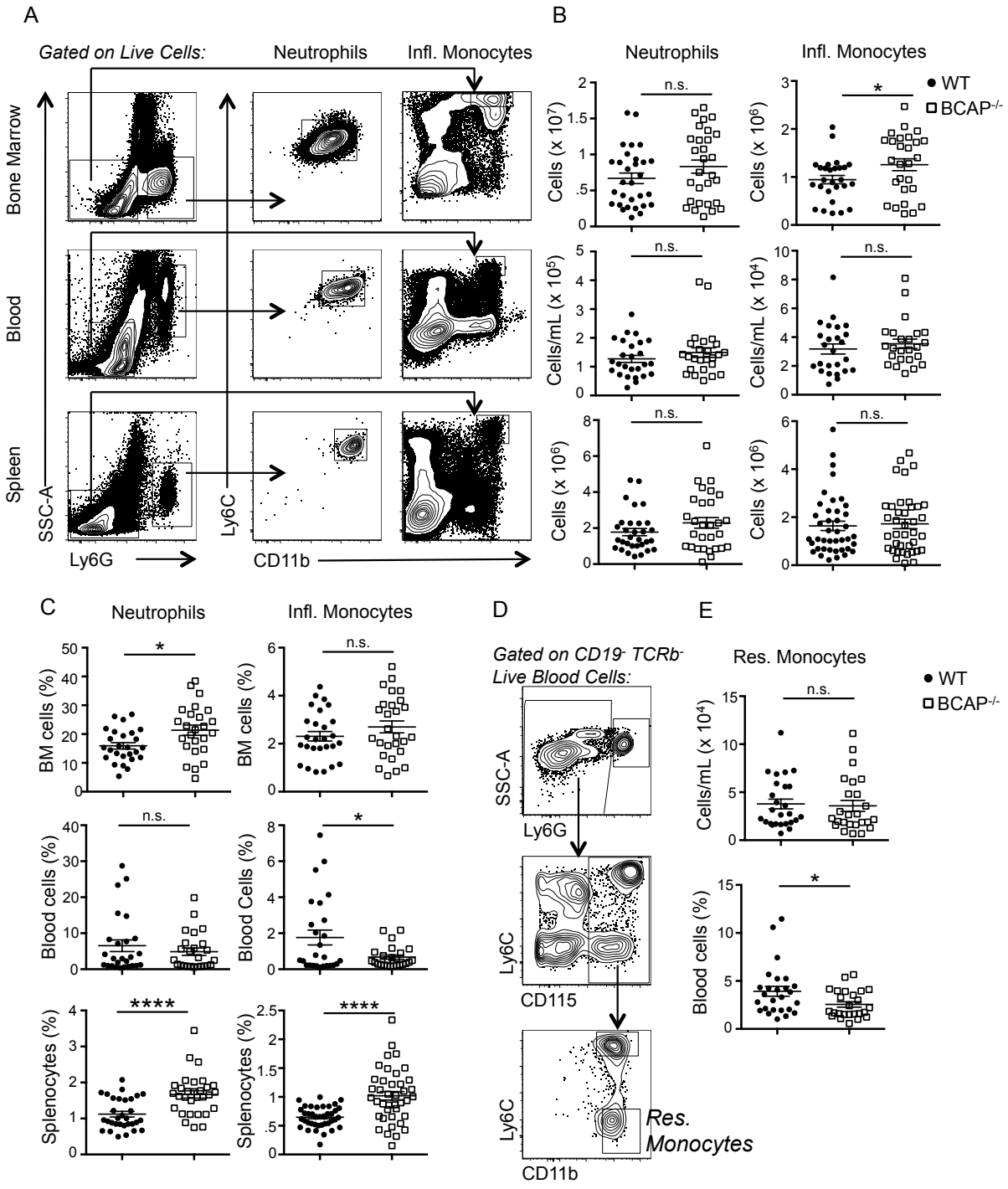


**Figure 2.1. Increased number of BM monocytes in BCAP$^{-/-}$ mice.** (A) Representative flow cytometry plots identifying neutrophils and inflammatory monocytes in the BM, blood and spleen of WT mice. Neutrophils were identified as Ly6G$^{+}$Ly6C$^{int}$CD11b$^{+}$ live cells and inflammatory monocytes were identified as Ly6G$^{-}$Ly6C$^{hi}$CD11b$^{+}$ live cells. Absolute numbers

(B) and frequencies (C) of neutrophils (left column) and inflammatory monocytes (right column) in the BM (top row), blood (middle row) and spleen (bottom row) of WT and BCAP$^{-/-}$ mice. BM absolute numbers were determined from two tibias and two femurs per mouse; data pooled from 7 independent experiments. Absolute numbers per mL blood were determined from 25 μL of blood; data pooled from 3 independent experiments. Spleen absolute numbers were calculated from total spleen cellularity; data pooled from 8 independent experiments. (D) Representative flow cytometry plots identifying resident monocytes in the blood in WT mice. Resident monocytes were identified as Ly6G$^{-}$CD115$^{+}$Ly6C$^{lo}$CD11b$^{+}$ live cells. (E) Absolute numbers and frequencies of resident monocytes in the blood of WT and BCAP$^{-/-}$ mice. Absolute numbers per mL blood were determined from 25 μL of blood; data pooled from 3 independent experiments. For all graphs, data show mean +/- SEM; each symbol represents data from an individual mouse. * $p< 0.05$, ** $p< 0.01$, *** $p< 0.001$, **** $p< 0.0001$, n.s., not significant, as determined by two-tailed, unpaired Student's *t* test.

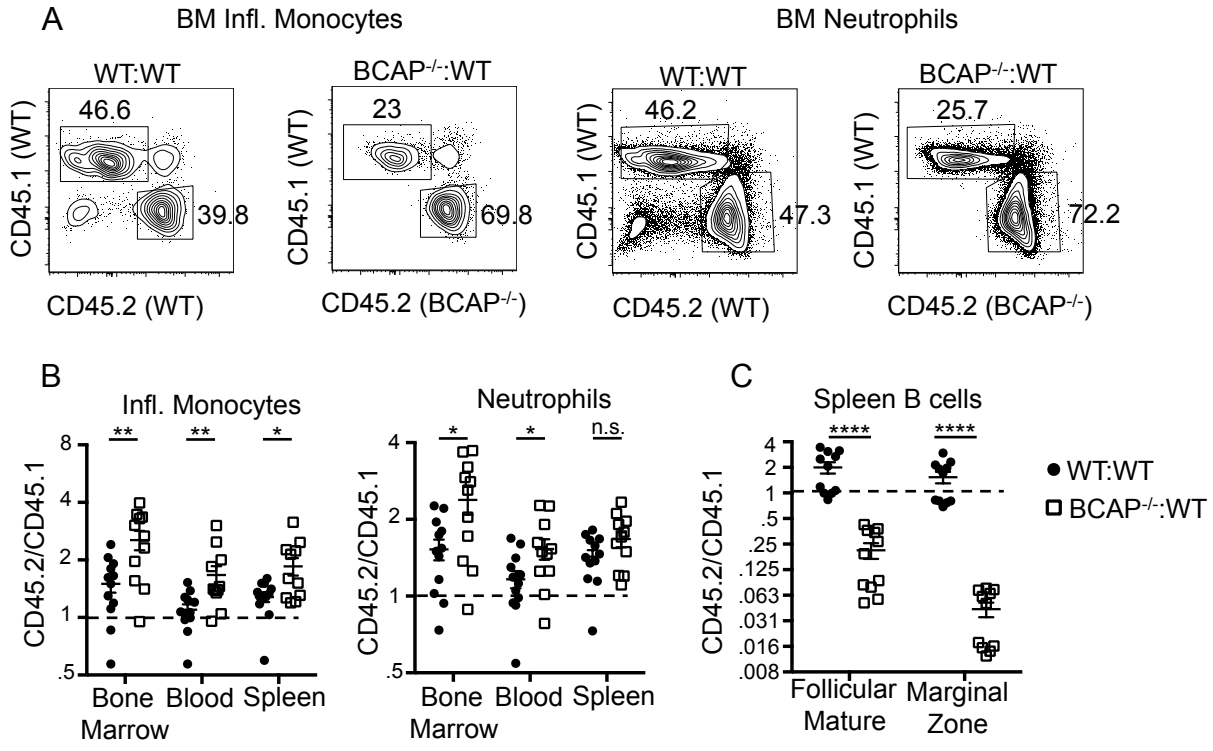


**Figure 2.2. BCAP differentially regulates myeloid and lymphoid cell development and/or homeostasis.** (A) Representative flow cytometry plots identifying $CD45.1^+$ and $CD45.2^+$ inflammatory monocytes and neutrophils in the BM of control mixed WT:WT and $BCAP^{-/-}$:WT BM chimeras reconstituted for >8 weeks; plots are representative of 3 independent experiments. Numbers represent frequency of $CD45.1^+$ or $CD45.2^+$ cells within indicated gated population. (B) Ratio of $CD45.2^+/CD45.1^+$ cells from WT:WT and $BCAP^{-/-}$:WT mixed chimeras; data pooled from 2 independent experiments. Inflammatory monocytes and neutrophils in were identified as in Supplementary Figure 1. (C) Ratio of $CD45.2^+/CD45.1^+$ cells from WT:WT and $BCAP^{-/-}$:WT mixed chimeras; data pooled from 2 independent experiments. Follicular mature B cells were identified as $CD19^+B220^+CD21^{hi}CD23^-$ live cells and marginal zone B cells as $CD19^+B220^+CD21^{int}CD23^+$ live cells. B and C show mean +/- SEM; each symbol represents data from an individual mouse, with n= 11 mice per group, and dotted lines represent a 1:1 reconstitution ratio. * $p< 0.05$, ** $p< 0.01$, *** $p< 0.001$, **** $p< 0.0001$, n.s., not significant, as determined by two-tailed, unpaired Student's *t* test.

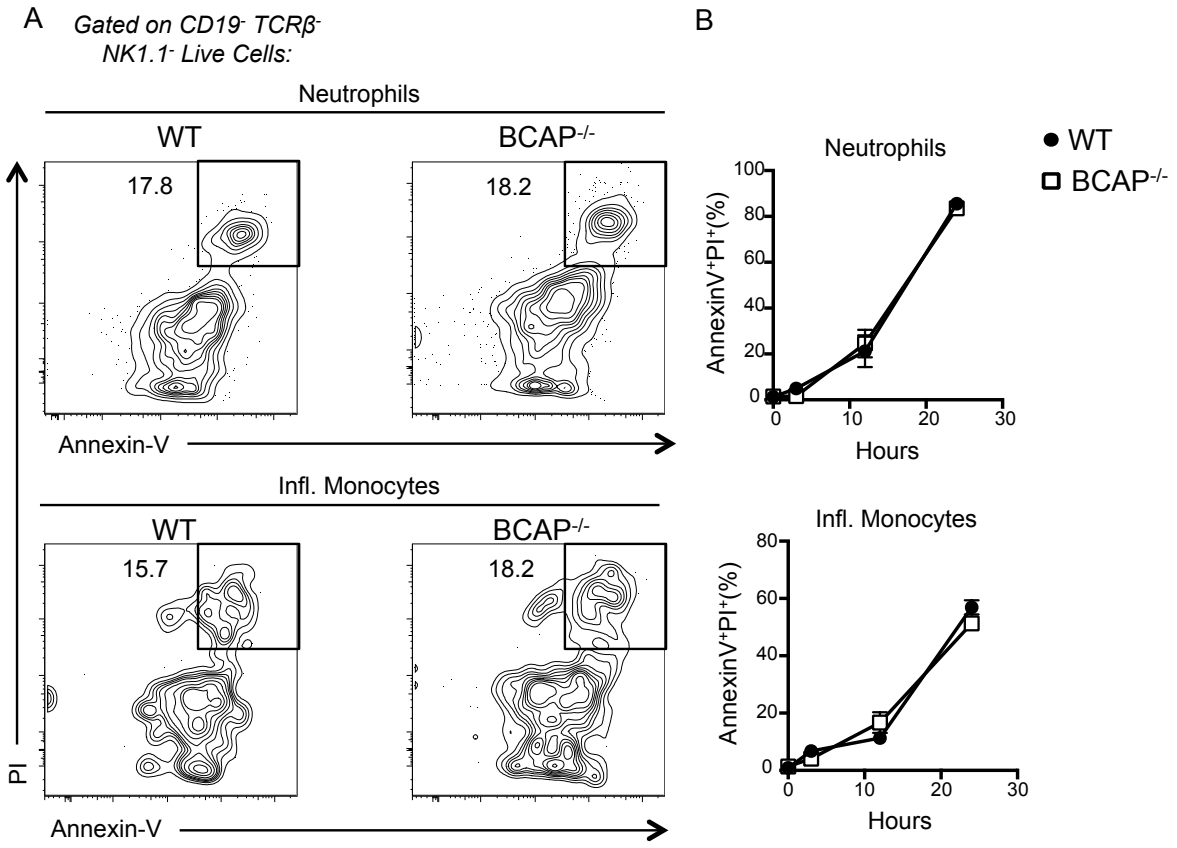


**Figure 2.3. Similar apoptosis in WT and BCAP$^{-/-}$ neutrophils and inflammatory monocytes.** (A) Representative flow cytometry plots identifying apoptotic cells among WT and BCAP$^{-/-}$ neutrophils (top) and monocytes (bottom) after ex vivo culture. 2 x $10^6$ CD19$^-$TCRβ$^-$NK1.1$^-$ cells were isolated from WT and BCAP$^{-/-}$ BM and cultured ex vivo for up to 24 hours at 37C. Upon harvest, neutrophils and monocytes were identified as Ly6G$^+$Ly6C$^+$CD11b$^+$ live cells and Ly6G$^-$Ly6C$^{hi}$CD11b$^+$ live cells, respectively, and apoptotic cells were identified by staining of both Annexin-V and Propidium Iodide (PI). (B) Graphs showing the frequencies of Annexin-V$^+$PI$^+$ neutrophils (top) and monocytes (bottom) at indicated times post-culture. Data are representative of 2 independent experiments, with n= 3 mice per group. For all graphs, data show mean +/- SEM. * $p< 0.05$, as determined by two-tailed, unpaired Student's *t* test.

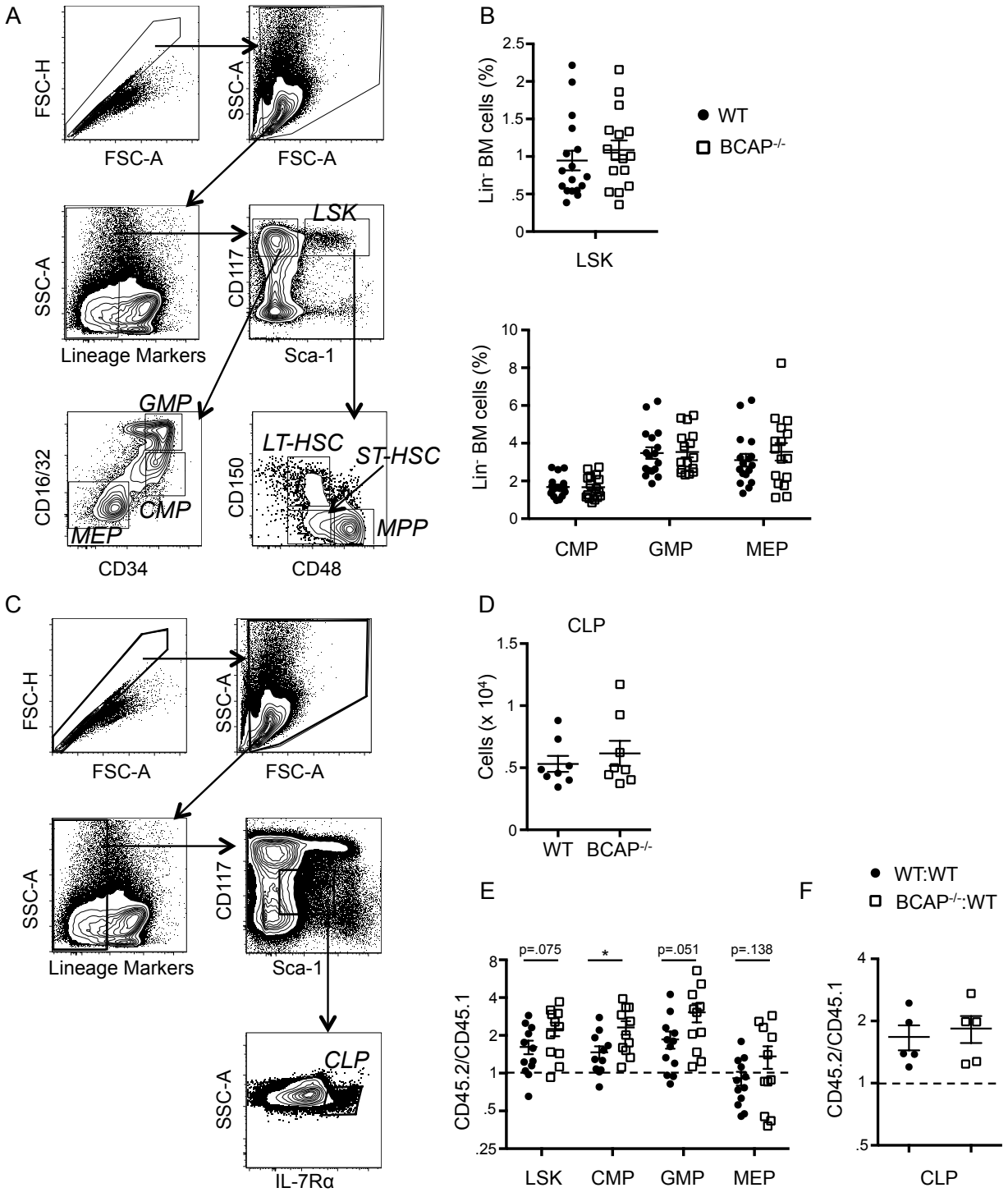


**Figure 2.4. Identification of BM HSPC populations.** (A) Identification of HSPC populations from Lineage$^-$ BM of WT mouse by flow cytometry. Cells were identified from live cell gating as follows: LSK (Lin$^-$CD117$^+$Sca1$^+$), LT-HSC (Lin$^-$CD117$^+$Sca1$^+$CD150$^+$CD48$^-$), ST-HSC (Lin$^-$CD117$^+$Sca1$^+$CD150$^-$CD48$^-$), MPP (Lin$^-$CD117$^+$Sca1$^+$CD150$^-$CD48$^+$), CMP (Lin$^-$CD117$^+$Sca1$^-$CD34$^+$CD16/32$^{int}$), GMP (Lin$^-$CD117$^+$Sca1$^+$CD34$^+$CD16/32$^{hi}$), MEP (Lin$^-$CD117$^+$Sca1$^-$CD34$^-$

CD16/32$^{lo}$). (B) Frequency of LSK (top), and CMP, GMP and MEP (bottom) cells within Lin$^-$ BM cells. Data are pooled from 4 independent experiments, with n= 16 mice per group. (C) Identification of CLP cells from Lineage$^-$ BM of WT mice by flow cytometry. CLP cells were identified as Lin$^-$CD117$^{int}$Sca1$^{int}$IL-7Rα$^+$ live cells. (D) Absolute numbers of CLP cells in WT and BCAP$^{-/-}$ Lin$^-$ BM; data are pooled from 2 independent experiments, with n= 8 mice per group. (E) Ratio of CD45.2$^+$/CD45.1$^+$ cells among the LSK, CMP, GMP and MEP populations from WT:WT and BCAP$^{-/-}$:WT mixed chimeras reconstituted for >8 weeks; data representative of 3 independent experiments. Each symbol represents data from an individual mouse, with n= 12 mice per group. (F) Ratio of CD45.2$^+$/CD45.1$^+$ CLP cells from WT:WT control and BCAP$^{-/-}$:WT mixed chimeras reconstituted for >8 weeks. Dotted line represents a 1:1 reconstitution ratio. Data are representative of 1 experiment, with n= 5 mice per group. For all graphs, data show mean +/- SEM; each symbol represents data from an individual mouse.

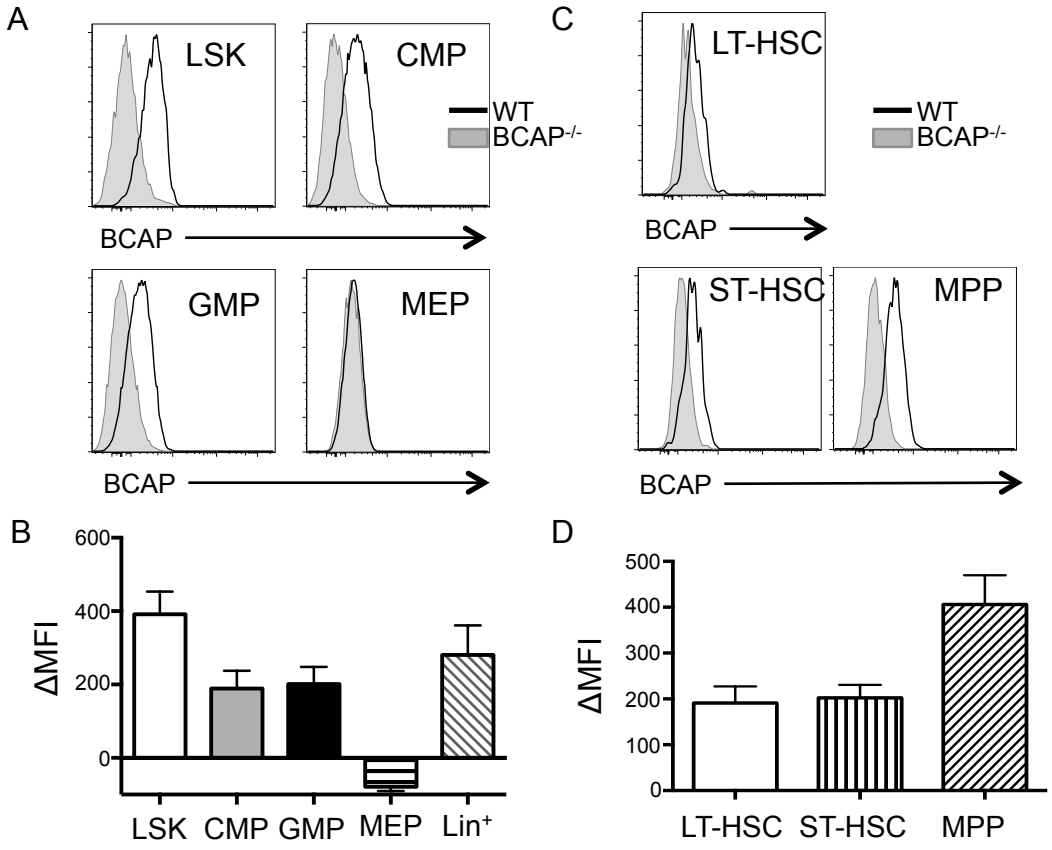


**Figure 2.5. BCAP is expressed within BM HSPC.** (A) Representative histograms of BCAP protein expression in LSK, CMP, GMP and MEP cells from WT (black, open histogram) and $BCAP^{-/-}$ (gray, shaded histogram) $Lin^-$ BM. $BCAP^{-/-}$ cells served as a negative control. HSPC populations were identified as in Supplementary Figure 3. (B) Change in BCAP staining Mean Fluorescence Index (ΔMFI) between WT and $BCAP^{-/-}$ cells. $Lineage^+$ cells served as a positive control for BCAP staining. ΔMFI was calculated as BCAP MFI in WT cells - BCAP MFI in $BCAP^{-/-}$ cells. (C) Representative histograms of BCAP protein expression in LT-HSC, ST-HSC and MPP cells from WT and $BCAP^{-/-}$ $Lin^-$ BM. (D) ΔMFI between WT and $BCAP^{-/-}$ cells. Graphs show mean + SEM of n= 3 mice per group. Data are representative of 3 independent experiments.

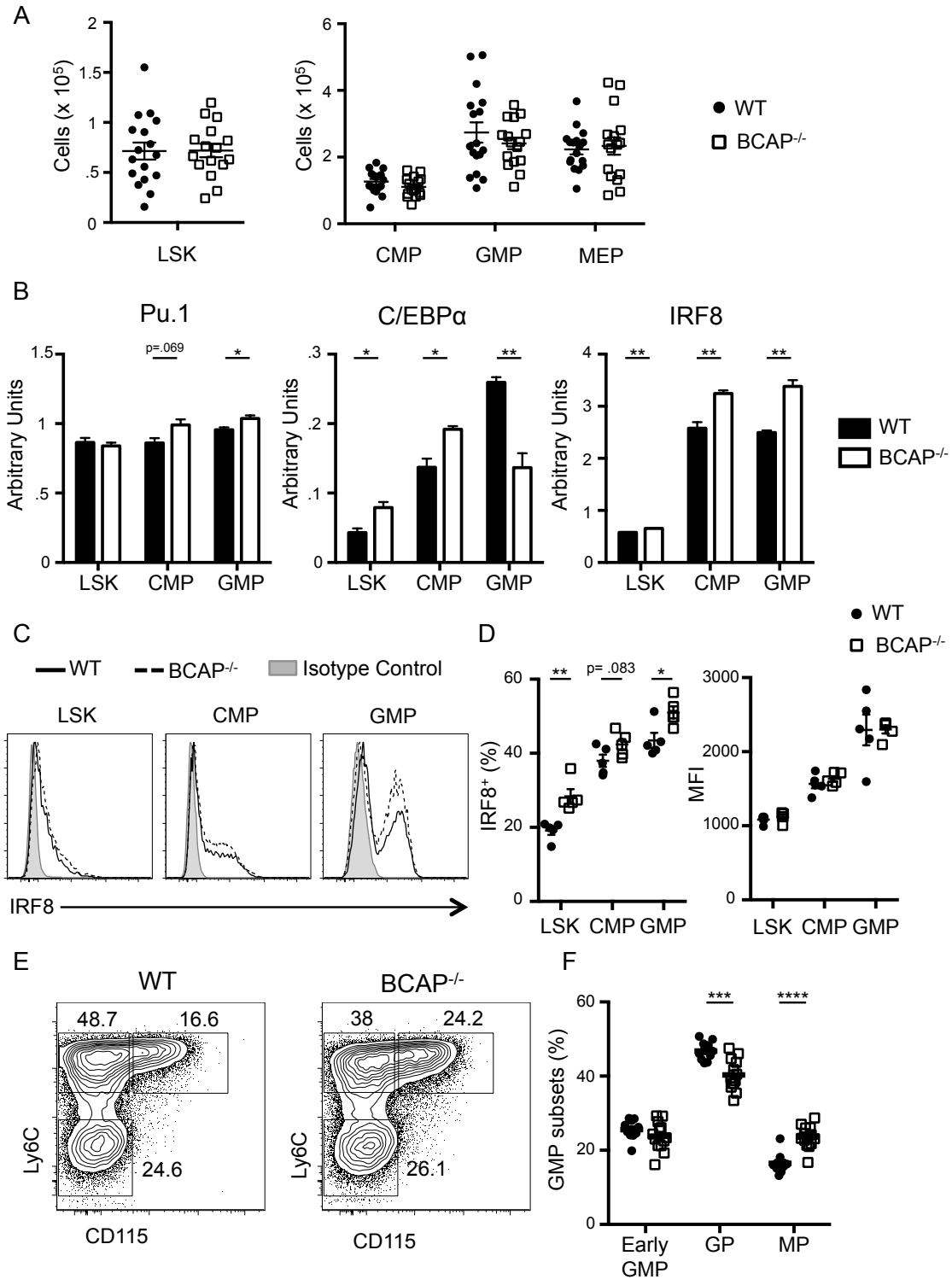


**Figure 2.6. BCAP$^{-/-}$ HSPC cells are primed for monocyte differentiation in the steady state.** (A) Absolute numbers of LSK (left) and CMP, GMP and MEP (right) cells in Lin$^-$ BM of WT and BCAP$^{-/-}$ mice. Data are pooled from 4 independent experiments, with n= 16 mice per group. (B) 100,000 LSK, 120,000 CMP, or 120,000 GMP cells were sorted from Lin$^-$ BM of 3 pooled

WT or BCAP$^{-/-}$ mice. mRNA was isolated from sorted cells, and reverse transcribed into cDNA. Relative expression of mRNA encoding Pu.1, C/EBPα, and IRF8 was determined by qRT-PCR from WT and BCAP$^{-/-}$ LSK, CMP, and GMP cells. Transcription factor expression was normalized to HPRT expression and shown as Arbitrary Units; graphs show mean + SD; data are representative of 3 independent experiments with n= 3 mice per group. (C) Representative flow plots of intranuclear staining for IRF8 or isotype control antibody in WT and BCAP$^{-/-}$ LSK, CMP and GMP. (D) Frequencies of IRF8$^{+}$ cells and Mean Fluorescence Index (MFI) for IRF8 staining in WT and BCAP$^{-/-}$ IRF8$^{+}$ LSK, CMP and GMP. (C-D) Data are representative of 2 independent experiments. Graphs show mean +/- SEM, with n= 5 mice per group. (E) Representative flow plots of GMP subsets identified by Ly6C and CD115 expression. GMP were gated as in Supplementary Figure 2 and then Early GMP (Ly6C$^{-}$CD115$^{-}$ GMP), GP (Ly6C$^{+}$CD115$^{-}$ GMP), and MP (Ly6C$^{+}$CD115$^{+}$ GMP) were identified as shown. (F) Frequencies of Early GMP, GP, and MP cells within the GMP population; data are pooled from 4 independent experiments, with n= 10 mice per group. For all graphs, data show mean +/- SEM; each symbol represents data from an individual mouse. * $p< 0.05$, ** $p< 0.01$, *** $p< 0.001$, **** $p< 0.0001$, as determined by two-tailed, unpaired Student's *t* test.

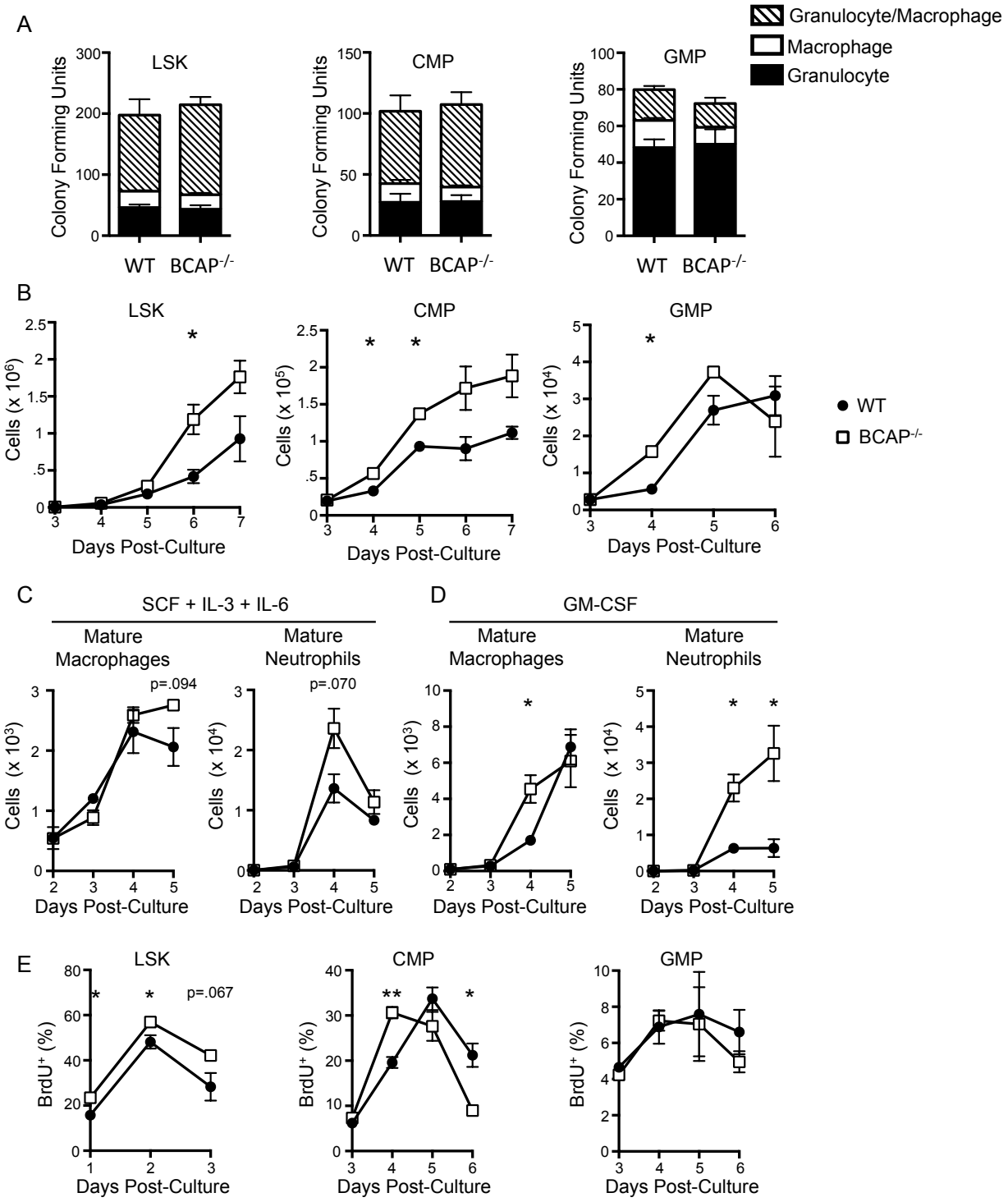


**Figure 2.7. BCAP$^{-/-}$ HSPC produce increased numbers of myeloid cells in vitro.** (A) Methylcellulose cultures were performed by sorting 250 LSK, CMP, or GMP from 3 individual WT and BCAP$^{-/-}$ mice into methylcellulose containing SCF, IL-3 and IL-6. After 5 days, differential Macrophage, Granulocyte, and mixed Macrophage/Granulocyte colony forming units were quantified. Data are pooled from two independent experiments with n= 6 mice per group.

(B) At indicated days, cells were harvested from LSK, CMP, and GMP methylcellulose cultures and quantified by flow cytometry. (C) Absolute numbers of mature macrophages (left) and mature neutrophils (right) from WT and $BCAP^{-/-}$ GMP methylcellulose cultures containing SCF, IL3 and IL-6 at various days post-culture. (D) Absolute numbers of mature macrophages (left) and mature neutrophils (right) from WT and $BCAP^{-/-}$ GMP methylcellulose cultures containing GM-CSF at various days post-culture. (E) 5000 LSK, 250 CMP, and 250 GMP cells were sorted from 3 individual WT or $BCAP^{-/-}$ mice into methylcellulose containing SCF, IL-3 and IL-6. At indicated days, progenitor-derived cells were harvested from methylcellulose and cultured in media containing 10 μg/mL BrdU. Cells were incubated at 37°C in BrdU-containing media for the following: 1 hour for LSK, 4 hours for CMP and GMP. Cells were then harvested, fixed, stained, and examined for BrdU incorporation by flow cytometry. Frequency of $BrdU^{+}$ cells from LSK, CMP, and GMP methylcellulose cultures at indicated days. (B-E) Data are representative of 2-3 independent experiments; all graphs show mean +/- SEM with n= 3 mice per group. * $p< 0.05$, ** $p< 0.01$, as determined by two-tailed, unpaired Student's t test.

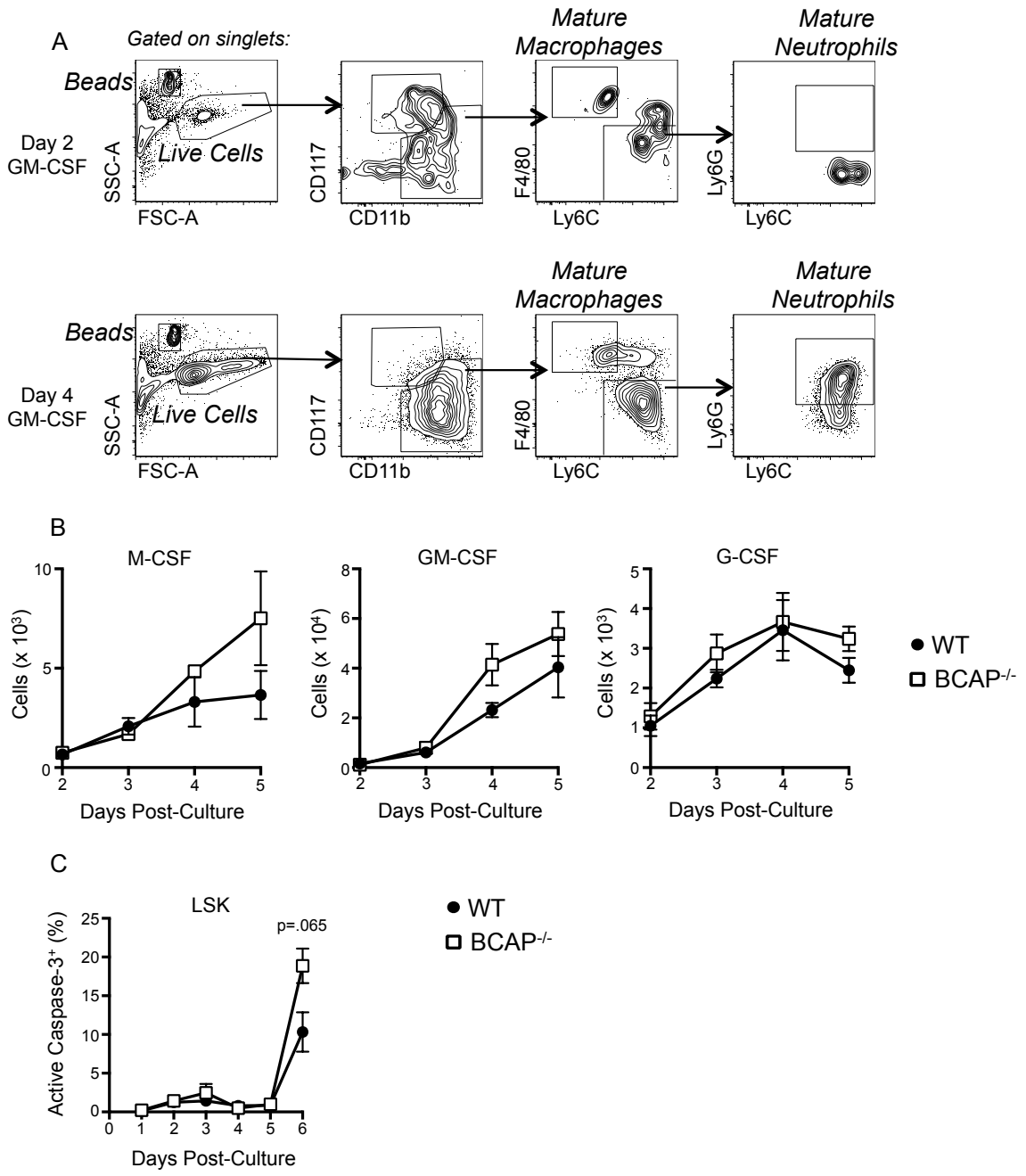


**Figure 2.8. Increased myeloid cell output from BCAP$^{-/-}$ progenitors.** (A) Representative flow cytometry plots identifying mature macrophages (CD117$^{-}$CD11b$^{+}$F4/80$^{+}$Ly6C$^{-}$Ly6G$^{+}$ live cells) and mature neutrophils (CD117$^{-}$CD11b$^{+}$F4/80$^{-}$Ly6C$^{+}$Ly6G$^{+}$ live cells) from methylcellulose cultures containing 50 ng/mL GM-CSF at 2 (top) and 4 (bottom) days post-culture. (B) 250 GMP were sorted into methylcellulose containing M-CSF, GM-CSF, or G-CSF. Cultures were harvested at indicated days and quantified by flow cytometry. Graphs show total cell yield each day and data are representative of 2-4 independent experiments with n= 3 mice per group. (C) Frequency of Active Caspase-3$^{+}$ cells in WT and BCAP$^{-/-}$ LSK methylcellulose cultures containing SCF, IL-3 and IL-6. Data representative of 2 independent experiments, with n= 3

mice per group. For all graphs, data show mean +/- SEM. * $p < 0.05$, as determined by two-tailed, unpaired Student's *t* test.

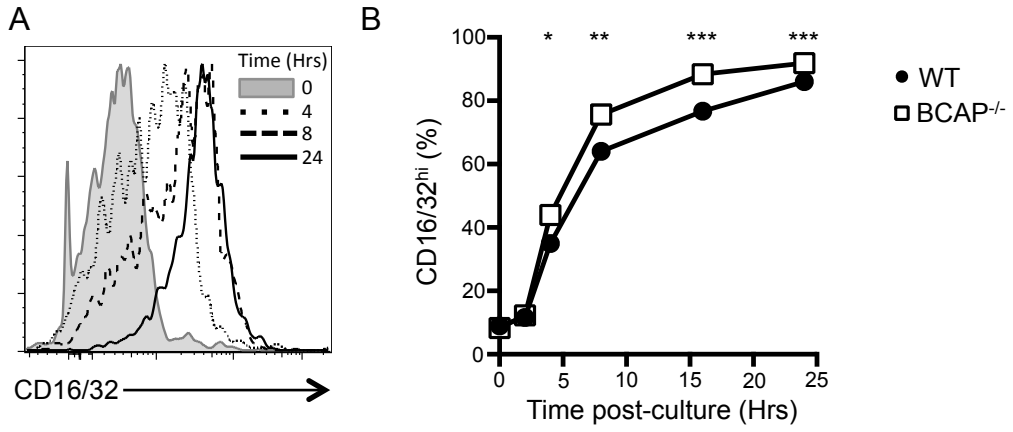


**Figure 2.9. Accelerated differentiation of BCAP$^{-/-}$ CMP cells in vitro.** (A) 5000 CMP cells from WT Lin$^{-}$ BM were cultured with SCF, IL-3, and IL-6 for up to 24 hours for maturation into GMP cells. Histogram overlay of CD16/32 expression on WT CMP cells at indicated times; data are representative of 2 independent experiments. B) Frequency of CD16/32$^{hi}$ cells at indicated times as in (A) from WT and BCAP$^{-/-}$ CMP cultures; data are representative of 2 independent experiments; data show mean of n= 3 mice per group; for all time points, SD < 3%. * $p< 0.05$, ** $p< 0.01$, *** $p< 0.001$, as determined by two-tailed, unpaired Student's *t* test.

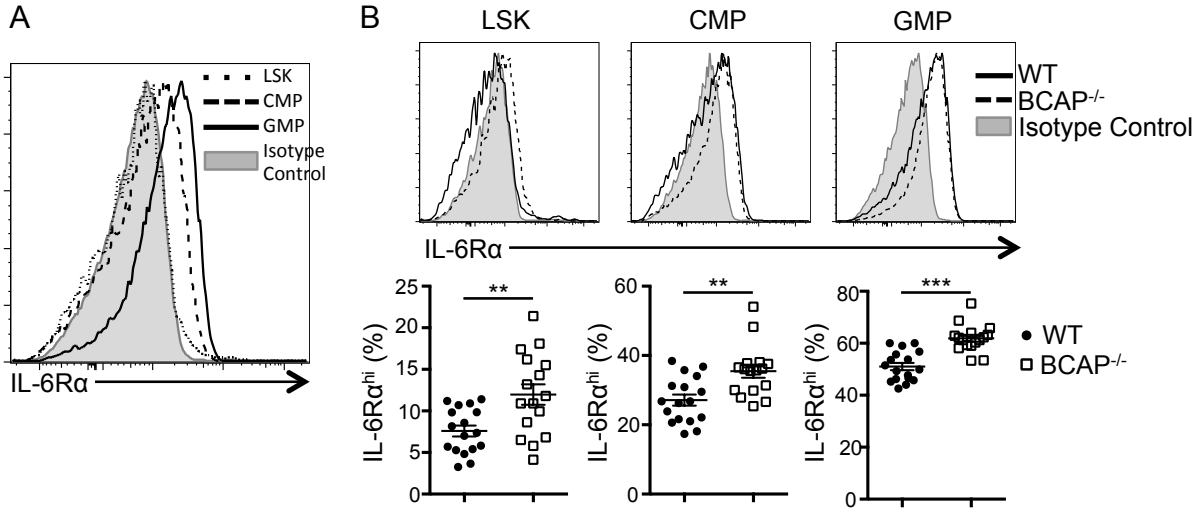


**Figure 2.10 Increased proportion of IL-6Rα$^{+}$ cells among BCAP$^{-/-}$ HSPC cells.** (A) Representative histogram overlay of IL-6Rα expression on LSK, CMP, and GMP cells in Lin$^{-}$ BM of WT mice. Data are representative of 4 independent experiments. (B) *Top*: Representative histogram overlays of IL-6Rα expression on LSK (left), CMP (middle), and GMP (right) cells from Lin$^{-}$ BM of WT and BCAP$^{-/-}$ mice; data are representative of 4 independent experiments. *Bottom*: Frequency of IL-6Rα$^{hi}$ cells within LSK (left), CMP (middle), and GMP (right) populations from Lin$^{-}$ BM of WT and BCAP$^{-/-}$ mice; data are pooled from 4 independent experiments and each symbol represents an individual mouse, graphs show mean +/- SEM, with n= 12 mice per group. (A-B) Isotype control antibody staining shown as gray shaded histograms. * $p< 0.05$, ** $p< 0.01$, *** $p< 0.001$, as determined by two-tailed, unpaired Student's *t* test.

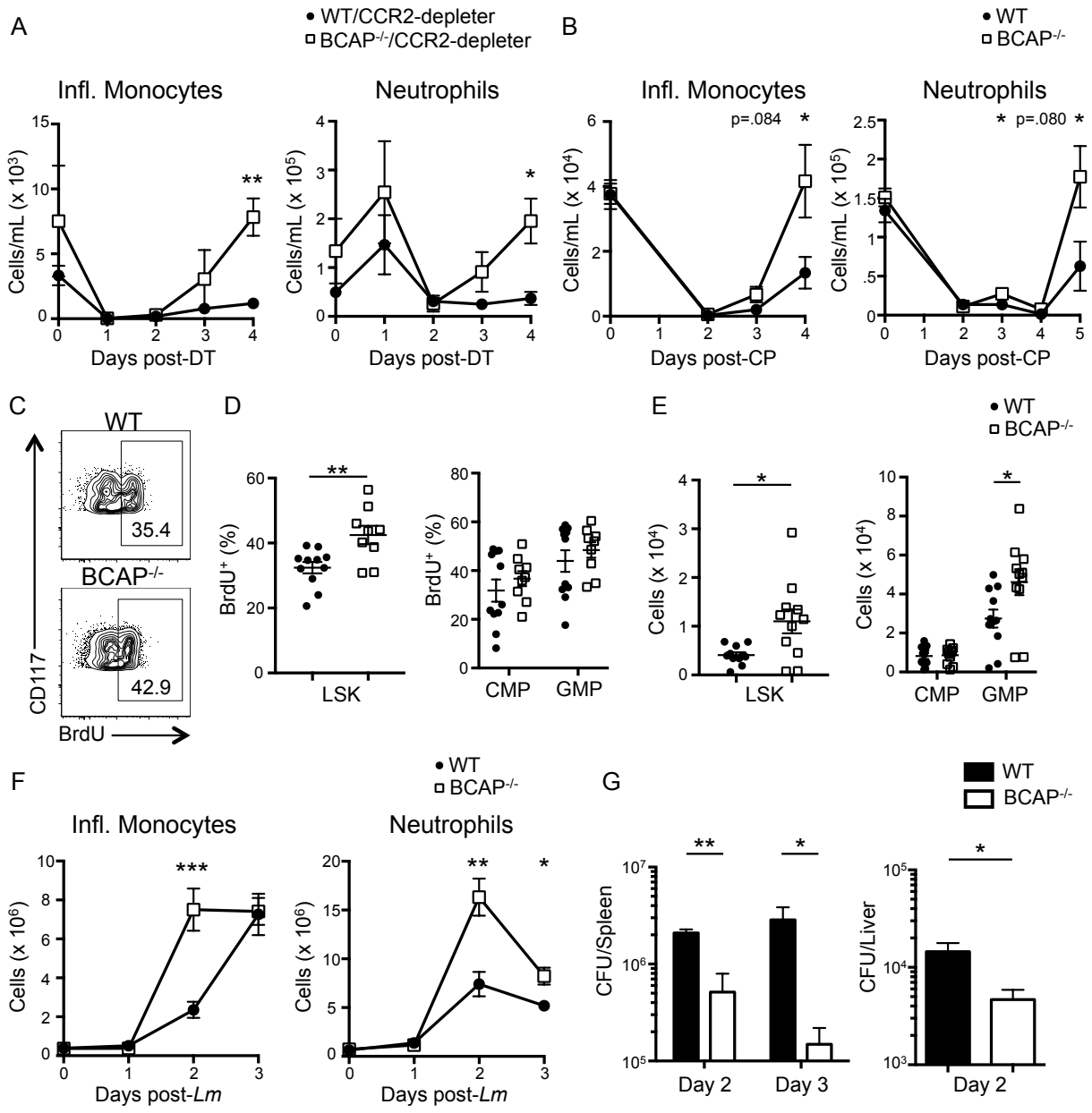


**Figure 2.11. BCAP$^{-/-}$ mice exhibit accelerated monocyte and neutrophil replenishment and/or accumulation during demand situations.** (A) Absolute number of inflammatory monocytes and neutrophils per mL of blood from WT/Ccr2-depleter and BCAP$^{-/-}$/Ccr2-depleter mice at the indicated times after Diphtheria Toxin (DT) treatment; data are representative of 3 independent experiments with n= 4 mice per group. (B) Absolute number of inflammatory monocytes and neutrophils per mL of blood from mice at the indicated time points after cyclophosphamide (CP) treatment; data are representative of 3 independent experiments with n= 10 mice per group. (C) Representative flow plots showing LSK from WT and BCAP$^{-/-}$ mice treated for 48 hours with cyclophosphamide, followed by 1 hour pulse i.p. with 1 mg BrdU. Numbers represent frequency of BrdU$^{+}$ cells within indicated population. (D) Frequencies of BrdU$^{+}$ LSK and GMP from WT and BCAP$^{-/-}$ mice 48 hours post-CP treatment. (E) Absolute

numbers of LSK, CMP and GMP in $Lin^-$ BM of WT and $BCAP^{-/-}$ mice 48 hours post-cyclophosphamide treatment. (C-E) Data represent 2 independent experiments with n= 11 mice per group. (F) Absolute number of inflammatory monocytes and neutrophils per spleen of mice at the indicated time points during *Listeria monocytogenes (Lm)* infection; data are representative of 3 independent experiments with n= 3-5 mice per group. Data show mean +/- SEM, and each symbol represents data from an individual mouse. (G) Graphs showing the number of *Lm* colony-forming units (CFU) present within the whole spleen and liver of WT and $BCAP^{-/-}$ mice at the indicated days post-*Listeria monocytogenes* infection. CFU were calculated and are shown as CFU per total organ. Graphs show mean +/- SEM, with n= 4 mice per group. * $p< 0.05$, ** $p< 0.01$, *** $p< 0.001$, as determined by two-tailed, unpaired Student's *t* test.

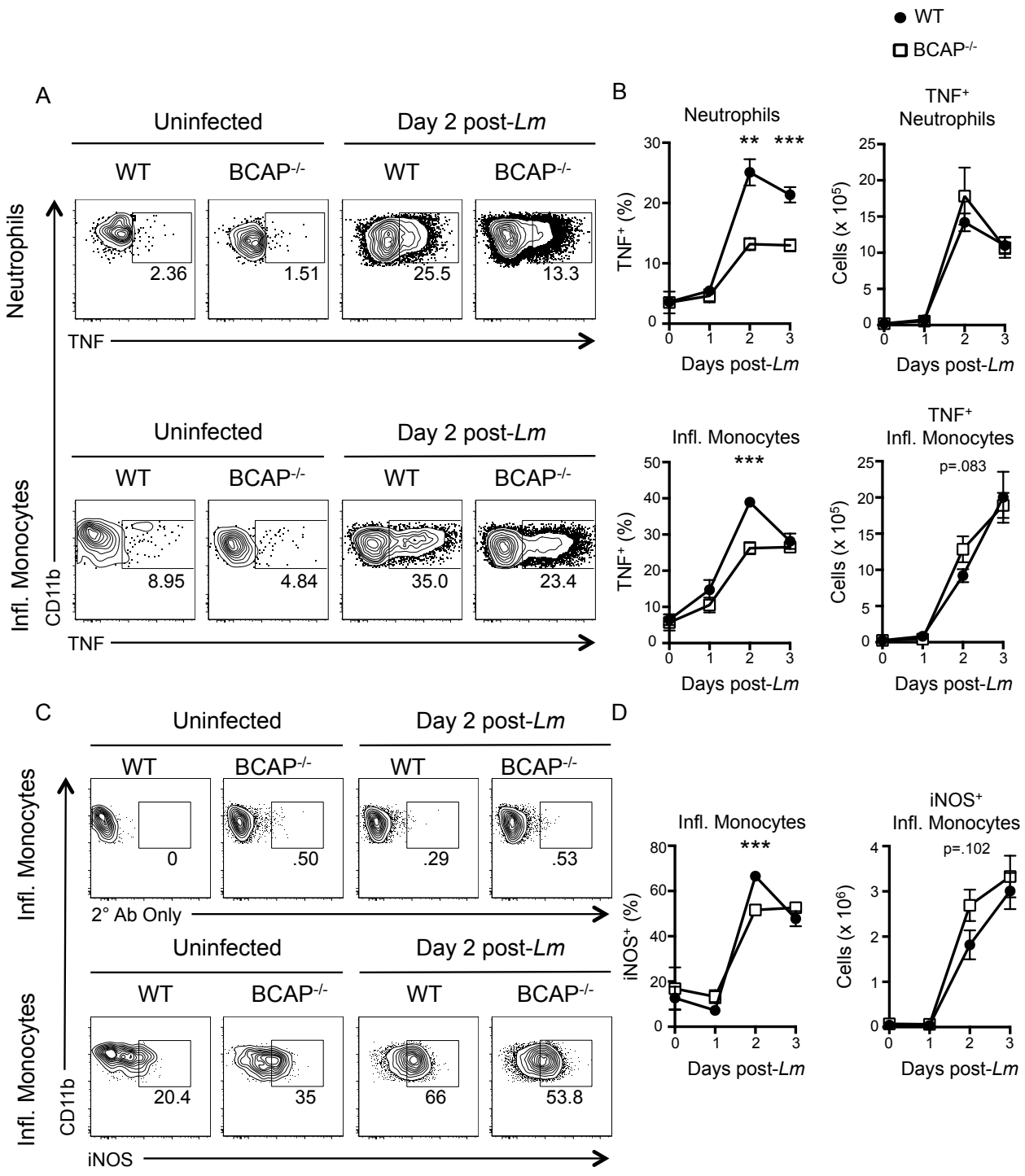


**Figure 2.12. Activation of neutrophils and inflammatory monocytes in WT and BCAP$^{-/-}$ mice during *Listeria monocytogenes* infection.** Mice were infected i.v. with 3000 CFU *Lm*. At days 1-3 post-*Lm*, spleens were harvested and digested, and 5 x $10^6$ splenocytes were incubated with brefeldin A for 4 hours, fixed, permeabilized, stained intracellularly for TNF or iNOS, and examined by flow cytometry. **(**A) Representative flow cytometry plots identifying TNF$^+$ cells among splenic neutrophils (top) and monocytes (bottom) from uninfected mice (left) and mice

infected with *Lm* for 2 days. (B) Graphs showing the frequency (left) of $TNF^+$ cells among splenic neutrophils (top) and monocytes (bottom) and the absolute number (right) of splenic $TNF^+$ neutrophils and monocytes at the indicated days post-*Lm* infection. (C) Representative flow cytometry plots showing intracellular staining for control (top) or iNOS (bottom) in inflammatory monocytes from uninfected mice and mice infected with *Lm* for 2 days. iNOS intracellular staining was conducted using a Rabbit anti-mouse iNOS antibody, followed by secondary staining with a PE-conjugated Goat anti-rabbit $F(ab')_2$ antibody. $iNOS^+$ cells were compared to control samples stained with the secondary PE-conjugated antibody alone. (D) Graphs showing the frequency of splenic monocytes staining for iNOS (left) and the absolute number of $iNOS^+$ inflammatory monocytes (right) at the indicated days post-*Lm* infection. Graphs show mean +/- SEM, with n= 5 mice per group. * $p< 0.05$, ** $p< 0.01$, *** $p< 0.001$, **** $p< 0.0001$ n.s., not significant, as determined by two-tailed, unpaired Student's *t* test.

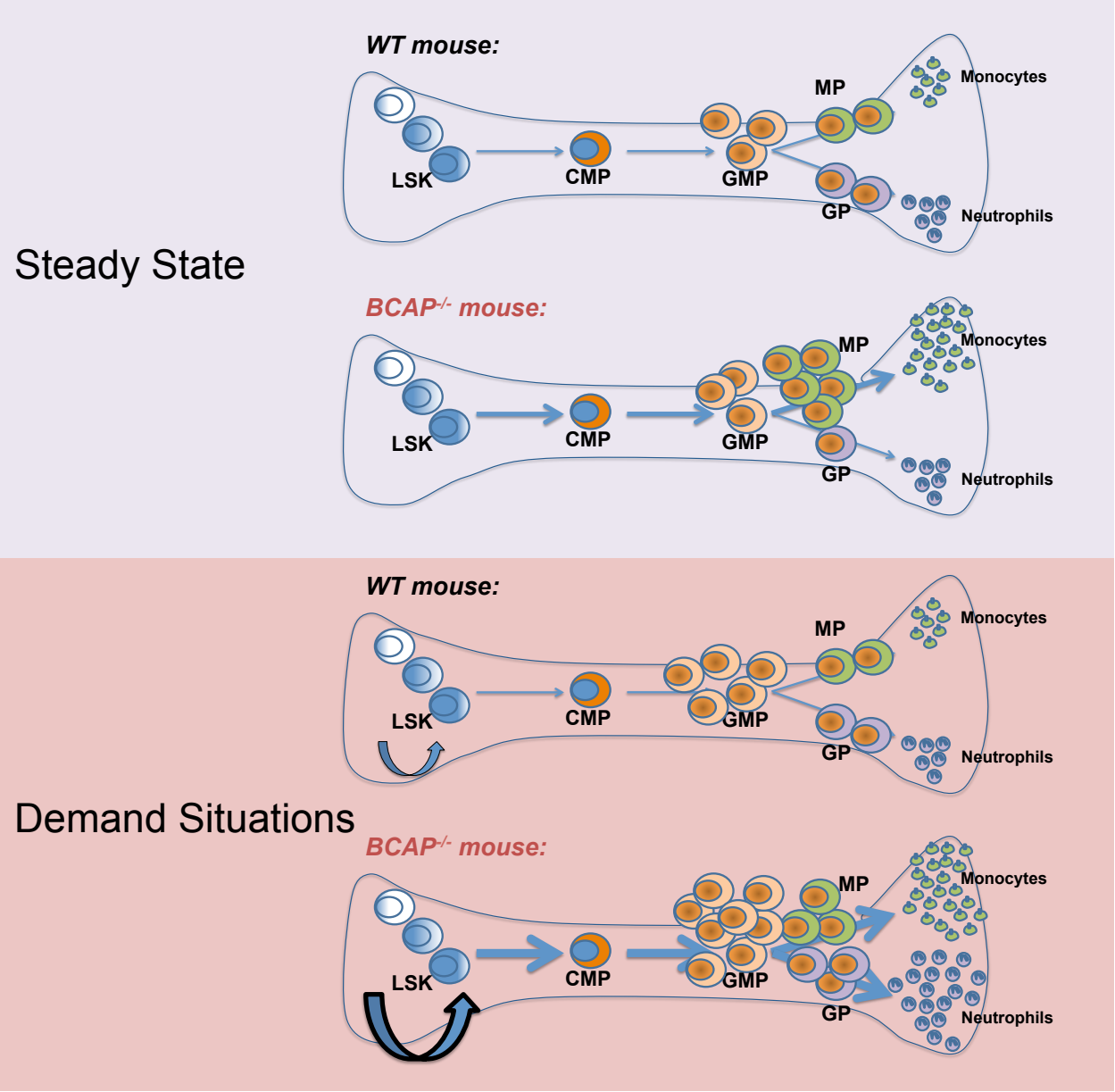


**Figure 2.13. Summary diagrams showing myelopoiesis in WT and BCAP$^{-/-}$ mice in the steady state and during demand situations.** Purple shaded box shows bone marrow myelopoiesis in the steady state. Red shaded box shows bone marrow myelopoiesis during situations of demand, including infection and myeloablation. Weight of arrows shows the magnitude of differentiation at each stage of myelopoiesis. Curved arrows show proliferation in the LSK compartment during demand situations.

# CHAPTER 3: BCAP ACT AS A POSITIVE REGULATOR OF HEMATOPOIETIC STEM CELL QUIESCENCE AND/OR SELF-RENEWAL

**Abstract**

BCAP is a signaling adaptor protein expressed in cells of the hematopoietic lineage, including the Long-Term Hematopoietic Stem cells (LT-HSC) in the bone marrow. Here we examined the role of BCAP in the homeostasis of the LT-HSC population, and its oligopotent downstream progeny, including the Short-Term Hematopoietic Stem cells (ST-HSC) and the Multipotent Progenitors (MPP). BCAP$^{-/-}$ mice had decreased numbers of LT-HSC in the bone marrow compared to WT mice at the steady state, suggesting that BCAP functions as a positive regulator of LT-HSC numbers. This is in contrast to the equal numbers of MPP in WT and BCAP$^{-/-}$ mice. Furthermore, BCAP$^{-/-}$ LT-HSC and MPP were hyper-proliferative compared to their WT counterparts in the steady state, as determined by BrdU incorporation. These data suggest that BCAP is critical for the quiescence or self-renewal of LT-HSC in the bone marrow. To further examine the impact of BCAP within the HSC compartment, we sorted WT and BCAP$^{-/-}$ LT- and ST-HSC and examined global gene expression via RNA sequencing. This resulted in identifying 274 genes differentially expressed in BCAP$^{-/-}$ LT- and ST-HSC compared to their WT counterparts, with 57 of these genes having a >2-fold change in expression in BCAP$^{-/-}$ HSC compared to WT HSC. These genes included transcription factors critical for hematopoiesis, MAP kinase signaling, insulin signaling, and Type I Interferon signaling. Lastly, BCAP$^{-/-}$ LT-HSC failed to replenish their numbers as well as WT LT-HSC after HSC transplantation into lethally irradiated mice, but were capable of producing similar frequencies of mature hematopoietic cells as WT LT-HSC after transplantation. Together, these data suggest that

BCAP may play a role in the quiescence and/or self-renewal of the LT-HSC, and therefore identifies a novel function for BCAP within the Hematopoietic Stem cell compartment.

**Introduction**

Long-Term Hematopoietic Stem cells (LT-HSC) represent the least-differentiated population among hematopoietic cells, and produce all the hematopoietic lineages throughout life[1,30]. Hematopoiesis drives differentiation of LT-HSC to ST-HSC, and subsequently to MPP cells, which lose self-renewal capacity, are highly proliferative, and differentiate into lineage-restricted progenitor cells. The LT-HSC pool must balance the ability to remain quiescent and the capacity to self-renew with their potential to proliferate and differentiate into the hematopoietic progenitors that produce the mature hematopoietic lineages. The control of these states is critical for both the steady production of new erythroid, lymphoid and myeloid cells throughout life, and also for adapting to rapidly respond to hematopoietic needs during demand situations, such as myeloablation and infection[5,69].

Many genes have been implicated to function in the quiescence and self-renewal ability of LT-HSC. These include transcription factors, components of signaling pathways, and genes involved in controlling cell cycling and proliferation[1,30,70]. Altering the expression or function of many of these genes leads to deleterious effects in mice, including hematopoietic malignancies, myeloproliferative disorders, and bone marrow failure after transplantation[70,71]. Therefore, identifying genes critical for maintaining both the capacity of LT-HSC to self-renew and for proliferation and lineage differentiation may lead to clinical interventions for patients undergoing transplantation.

As previously described, we have identified BCAP as an inhibitor of myelopoiesis in LSK cells in both the steady state and during demand situations[72]. Additionally, BCAP is expressed within the LT-HSC population within the bone marrow, suggesting that BCAP functions within the LT-HSC. Furthermore, we found that $BCAP^{-/-}$ LT-HSC did not reconstitute

the HSC pool as well as WT LT-HSC in HSC after transplantation into lethally irradiated mice, further showing that BCAP is a critical regulator for HSC maintenance. Therefore, we examined whether BCAP was important for the homeostasis of the LT-HSC population.

## Materials and Methods

### Mice, BM chimeras and in vivo treatments

All mice were bred at the Benaroya Research Institute, and C57BL/6 mice were also purchased from Jackson Laboratories. BCAP$^{-/-}$ mice[37] with a disrupted *Pik3ap1* gene were back-crossed nine generations to C57BL/6 background. All experiments were performed under an IACUC-approved protocol.

HSC transplant mice were generated by lethally irradiating (1000 rad) recipient C57BL/6 x B6.SJL F1 (CD45.1$^{+}$ CD45.2$^{+}$) mice and reconstituting with 250 sorted LT-HSC from the BM of either WT (CD45.2$^{+}$) or BCAP$^{-/-}$ (CD45.2$^{+}$) mice and 2.5 x $10^5$ whole BM cells from B6.SJL (CD45.1$^{+}$) mice.

For proliferation, mice were injected i.p. with 1 mg/mL BrdU for 1 hour. BrdU incorporation was assayed using the BD BrdU Flow Kit (BD Biosciences).

### Cell isolation and staining

Mouse BM cells were isolated and stained with antibodies for flow cytometry as previously described[8,17,72]. Lineage$^{-}$ BM cells were isolated using a Lineage Cell Depletion Kit (Miltenyi Biotec). All mAbs used for flow cytometry are listed in Table 2.1. Data were acquired using an LSR II or FACSCanto (BD Biosciences) and analyzed using FlowJo software (TreeStar). Doublets were excluded from live cell gating using forward light scatter and side scatter. Cell sorting was conducted using a FACSAria II (BD Biosciences). Cells were quantified by flow cytometry using polystyrene counting beads (Polysciences).

### cDNA amplification and RNA sequencing

cDNA was reverse transcribed from mRNA from 750 sorted LT-HSC and 750 sorted ST-HSC from WT or BCAP$^{-/-}$ BM using a SMARTer cDNA synthesis kit (Takara). LT-HSC were

sorted from 4 individual WT and 4 individual BCAP$^{-/-}$ mice using a FACSAria II system (BD Biosciences). RNA sequencing of cDNA libraries was conducted by the Genomics Core at the Benaroya Research Institute.

**Bioinformatics and Statistics**

For Figures 3.1-3.2 and 3.4, data were analyzed by Student's unpaired *t* test using Prism (GraphPad). RNA sequencing analysis was completed by the Bioinformatics Core at the Benaroya Research Institute. Raw RNA-seq data was processed and aligned to the GRCm37/mm9 reference genome with bowtie and TopHat. Read counts were generated using htseq-count. Quality control cutoffs for each cDNA library examined by RNA-seq included the following: $> 1 \times 10^6$ total FASTQ reads, >80% aligned reads to genome, < 1.0 median CV coverage (calculated by Picard). Potential confounding variables that drove variance in the data were removed by Surrogate Variable Analysis with the sva package. Identification of significantly differentially expressed genes was identified between WT and BCAP$^{-/-}$ HSC using the following variables: BCAP gene status, combined population of LT- and ST-HSC, and RNA concentration.

## Results

### BCAP$^{-/-}$ mice have decreased numbers of LT-HSC in the BM

As previously described, BCAP$^{-/-}$ mice had similar frequencies and numbers of BM HSPC in the steady state, including within the LSK population (Figure 2.6). Due to the LSK population being composed of the LT-HSC, ST-HSC and MPP cells, we therefore utilized the markers CD150 and CD48 to distinguish these populations among LSK cells in WT and BCAP$^{-/-}$ mice (Figure 3.1A). When examining the frequency among Lineage$^{-}$ BM cells, BCAP$^{-/-}$ mice trended towards a lower frequency of LT-HSC compared to WT mice (Figure 3.1B). In contrast, WT and BCAP$^{-/-}$ mice had similar frequencies of ST-HSC and MPP cells. When examining absolute numbers of these populations within the BM, we found that BCAP$^{-/-}$ mice had significantly fewer LT-HSC compared to WT mice (Figure 3.1C). BCAP$^{-/-}$ BM also exhibited a trend towards fewer ST-HSC compared to WT BM. In contrast, WT and BCAP$^{-/-}$ BM had similar numbers of MPP cells. Therefore, BCAP$^{-/-}$ mice have decreased numbers of HSC, suggesting that BCAP is involved in the homeostasis of the HSC populations.

### BCAP$^{-/-}$ LT-HSC and MPP are hyper-proliferative in the steady state

We next asked whether this decreased LT-HSC number in BCAP$^{-/-}$ mice coincided with alterations in the steady-state proliferation of the LSK populations. Using BrdU incorporation as a measure of proliferation, we found that BCAP$^{-/-}$ LT-HSC had significantly increased uptake of BrdU compared to their WT counterparts (Figure 3.2A-B). BrdU incorporation in the ST-HSC population was similar between WT and BCAP$^{-/-}$ mice. Furthermore, BCAP$^{-/-}$ MPP also exhibited increased uptake of BrdU compared to WT MPP. This increase in proliferation within the LT-HSC population in BCAP$^{-/-}$ mice suggests that BCAP inhibits the proliferation of LT-HSCs, and thus may promote quiescence and/or self-renewal capacity in the HSC compartment.

Furthermore, BCAP also restricts proliferation at the MPP stage, showing that the role of BCAP in progenitor proliferation occurs throughout early hematopoietic differentiation.

**Global alterations in gene expression in BCAP$^{-/-}$ HSC**

With the exception of the PI3K pathway, the signaling pathways that BCAP associates with remain unclear. Therefore, to examine the impact of BCAP within the HSC compartment, we examined global gene expression via sequencing of RNA isolated from sorted LT- and ST-HSC from WT and BCAP$^{-/-}$ mice. The analysis of RNA from WT and BCAP$^{-/-}$ HSC yielded a total of 274 significantly differentially expressed genes in BCAP$^{-/-}$ HSC compared to WT HSC (Figure 3.3, Table 3.1). Of these 274 genes, 57 genes showed > 2 fold change difference between WT and BCAP$^{-/-}$ HSC. A wide array of genes involved in signaling pathways and cellular processes were represented within these 274 genes. These include genes involved in MAPK signaling (*Map3k1, Braf, Fosb, Jun, Junb, Jund*), Wnt/β-catenin signaling (*Dvl3, Tcf7l2, Ccnd2*), Insulin-like Growth Factor signaling (*Igf1r, Grb10*), and Type I Interferon signaling and responses (*Stat1, Oas2, Oas1a, Ifi27, Ly6a, Irf2, Irf2bp2*). Furthermore, several transcription factors known to function within HSC were differentially regulated in BCAP$^{-/-}$ cells, including *Sp1, Runx1, Gata2, and Egr1*. Only 40 of the 274 genes exhibited increased expression within BCAP$^{-/-}$ HSC. Interestingly, this subset included several genes downstream of Type I Interferon signaling (*Stat1, Oas1a, Oas2, Ifi27, Ly6a*), suggesting that BCAP$^{-/-}$ HSC may be hypersensitive to Type I Interferon signaling, which has previously been shown to drive HSC out of quiescence and promote myeloid differentiation during hematopoiesis[16,73]. Examining the 234 genes showing decreased expression in BCAP$^{-/-}$ HSC revealed the gene for BCAP itself (*Pik3ap1*), as well as additional genes involved in PI3K signaling (*Inpp4a, Pten*). Interestingly, both *Inpp4a* and *Pten* negatively regulate the PI3K pathway, suggesting that PI3K signaling is altered in HSC

in the absence of BCAP, potentially to compensate for diminished PI3K activation in BCAP$^{-/-}$ HSC. Furthermore, BCAP$^{-/-}$ HSC exhibited decreased expression of *Irf2*, a known antagonist of the Type I Interferon pathway[73], as well as a promoter of HSC quiescence. Overall, genes controlling multiple cellular functions and signaling pathways are altered in BCAP$^{-/-}$ HSC, further showing that BCAP functions in the homeostasis of the HSC compartment in the BM.

**Diminished HSC compartment reconstitution in BCAP$^{-/-}$ HSC transplant mice**

To better test the fitness of BCAP$^{-/-}$ LT-HSC, we made HSC transplant mice[74,75] by transferring 250 LT-HSC from WT or BCAP$^{-/-}$ (CD45.2$^{+}$) mice with 2.5 x $10^5$ whole BM cells (CD45.1$^{+}$) into lethally irradiated F1 recipient mice (CD45.1$^{+}$CD45.2$^{+}$) followed by reconstitution for >12 weeks (Figure 3.4A). By 12 weeks post-transplantation, we found similar reconstitution of B cells, T cells, neutrophils and inflammatory monocytes in the blood of WT and BCAP$^{-/-}$ HSC transplant mice (Figure 3.4B), showing that BCAP$^{-/-}$ LT-HSC are as capable as WT LT-HSC to reconstitute the myeloid and lymphoid cells after transfer. However, when examining the HSPC populations in the BM at 25 weeks post transplantation, we found BCAP$^{-/-}$ transplant mice had a trend towards lower frequency of donor-derived LT-HSC and MPP, and a significantly decreased frequency of donor-derived ST-HSC compared to WT transplant mice (Figure 3.4C). Similarly decreased frequencies of donor-derived CMP, GMP and MEP were found in BCAP$^{-/-}$ transplant mice compared to their WT counterparts (Figure 3.4D). Therefore, while BCAP$^{-/-}$ LT-HSC are as capable as WT LT-HSC in reconstituting the mature hematopoietic populations, BCAP$^{-/-}$ LT-HSC are incapable of regenerating the HSPC pool as well as WT LT-HSC, further indicating that BCAP promotes the maintenance of the HSC pool in the BM.

**Discussion**

Here we have identified a novel role for BCAP as a regulator of LT-HSC homeostasis within the BM of adult mice. BCAP$^{-/-}$ mice had fewer LT-HSC in their BM, as well as a concomitant increase in LT-HSC proliferation compared to the LT-HSC in WT mice. Furthermore, we identified 274 differentially expressed genes in the HSC compartment of BCAP$^{-/-}$ mice compared to their WT counterparts. Additionally, BCAP$^{-/-}$ LT-HSC exhibited diminished reconstitution of the BM HSC pool compared to WT LT-HSC in HSC transplant mice. Overall, these data suggest that BCAP serves as a positive regulator of LT-HSC quiescence and/or self-renewal, and a negative regulator of HSC proliferation.

The increased proliferation of LT-HSC and MPP is likely related to the decreased LT-HSC pool size in BCAP$^{-/-}$ mice, as proliferation of LT-HSC is linked to their differentiation out of the quiescent population of HSC. Therefore, the increased proliferation in BCAP$^{-/-}$ HSC correlates with the increased ability of BCAP$^{-/-}$ HSPC to produce myeloid cells[72], and further suggests that BCAP maintains HSC quiescence by limiting their ability to proliferate and begin differentiating into more restricted progenitor cells. The increased proliferation in LT-HSC and MPP cells correlates with the selective advantage of BCAP$^{-/-}$ myeloid progenitors, monocytes and neutrophils in mixed BM chimeras (Figure 2.2), rapid differentiation of BCAP$^{-/-}$ CMP to GMP cells (Figure 2.9), and the increased proportion of IL-6R$\alpha^{+}$ cells in BCAP$^{-/-}$ mice (Figure 2.10). Furthermore, the increased proliferation in steady state BCAP$^{-/-}$ LT-HSC and MPP is enhanced during demand situations both in vitro and in vivo, as BCAP$^{-/-}$ LSK cells are hyper-proliferative within methylcellulose cultures (Figure 2.7) and after cyclophosphamide-induced

myeloablation (Figure 2.11). Therefore, the increased myeloid cell differentiation capacity of BCAP$^{-/-}$ HSPC coincides with increased proliferation in the LT-HSC population.

RNA sequencing revealed a diverse array of genes that are differentially regulated within the LT- and ST-HSC in BCAP$^{-/-}$ BM. These included multiple pathways important for hematopoietic differentiation and function, both by promoting and inhibiting HSC proliferation. The transcription factors *Runx1*[76], *Sp1*[77], *Gata2*[36] and *Egr1*[78] all play critical roles in LT-HSC self-renewal and control HSC proliferation. Thus, decreased expression of these transcription factors in BCAP$^{-/-}$ HSC supports a role for BCAP in HSC maintenance. The role of the Wnt/β-catenin pathway during hematopoiesis is complex, as low levels of Wnt activation promote HSC self-renewal, intermediate signaling drive enhanced myelopoiesis, and high Wnt signaling cause HSC depletion[79,80]. Interestingly, we observed decreased expression of several members of the Wnt/β-catenin signaling pathway in BCAP$^{-/-}$ HSC, including the genes *Dvl3, Tcf712, and Ccnd2*. These data suggest that the absence of BCAP possibly causes reduced Wnt signaling and, therefore, the enhanced myelopoiesis observed in BCAP$^{-/-}$ mice.

BCAP$^{-/-}$ HSC had decreased expression of *Irf2*, an inhibitor of Type I Interferon signaling[73], and increased expression of several Type I Interferon signaling components and downstream targets, including *Stat1, Oas1a, Oas2, Ifi27, Ly6a, Irf2, Irf2bp2*. Previously, Type I Interferon signaling has been shown to promote the cycling of HSC to drive progenitor expansion and increased hematopoietic cell output[8,16], and this HSC cycling is inhibited by IRF2[73]. Therefore, our data suggest a role for BCAP in inhibiting Type I Interferon signaling by promoting IRF2 expression, thereby inhibiting HSC proliferation.

We additionally saw decreased expression in several pathways known to promote HSC maintenance. BCAP$^{-/-}$ HSC had decreased expression of several genes involved in MAPK

signaling, including *Map3k1, Braf, Fosb, Jun, Junb, and Jund*, which is known to promote HSC proliferation and therefore diminish HSC self-renewal[81]. Genes involved in Insulin/Insulin-like Growth Factor signaling, which promote hematopoietic differentiation from HSPC[82], also exhibited decreased expression in BCAP$^{-/-}$ HSC. Together, these differences in gene expression observed by RNA sequencing suggest that BCAP may interact with multiple pathways, either by promoting or inhibiting HSC proliferation, with the aggregate result yielding a decreased number of LT-HSC and increased proliferation within the HSC compartment.

Along with its functions in mature hematopoietic cells, the PI3K-Akt pathway plays a number of functions during hematopoiesis. PI3K is activated downstream of multiple cytokines stimulating HSPC differentiation, including SCF[83], GM-CSF[22], and IL-3[84]. PI3K signaling has been shown to promote proliferation and differentiation of HSPC, and particularly supports myeloid differentiation[68]. Additionally, mice deficient in both AKT1 and AKT2, the downstream targets of PI3K activation, showed increased HSC quiescence, and decreased ability to differentiate into mature hematopoietic cells[85]. Therefore, PI3K signaling promotes HSC proliferation and differentiation. Interestingly, the reported phenotype of AKT1$^{-/-}$AKT2$^{-/-}$ LT-HSC, in which LT-HSC are more quiescent and fail to enter the cell cycle, is unlike that of BCAP$^{-/-}$ LT-HSC, as BCAP$^{-/-}$ LT-HSC had increased proliferation despite lacking BCAP, an adaptor that promotes PI3K activation. Therefore, the difference in these phenotypes suggests that BCAP may have a function in the HSC compartment that is independent of PI3K activation. Although no PI3K-independent functions have been identified for BCAP, the broad array of protein-protein interaction domains present in BCAP, as well as proteomic identification of BCAP-interacting proteins found in macrophages (Ni, James and Hamerman unpublished observations), indicates that BCAP performs multiple functions outside of PI3K activation.

Conversely, the absence of BCAP may lead to the increased activation of the PI3K pathway via other mechanisms. This is supported by decreased expression of two critical inhibitors of PI3K activation, *Pten* and *Inpp4a*, in BCAP$^{-/-}$ LT-HSC (Table 3.1). However, we observed similar phosphorylation of the PI3K/mTOR target ribosomal protein S6 in WT and BCAP$^{-/-}$ cells produced from cultured HSPC (J.M. Duggan and J.A. Hamerman, unpublished observations), suggesting that BCAP may not modulate PI3K activation in HSPC. Further examination into the proteins directly interacting with BCAP will provide a greater understanding of the pathways BCAP regulates to modulate the LT-HSC population and hematopoietic differentiation.

The factors controlling the LT-HSC population size remain unclear. While LT-HSC are capable of repopulating the hematopoietic lineages after lethal irradiation of mice[30], it remains unclear how critical the LT-HSC population is during steady state hematopoiesis. Recently, it was reported that upon depletion of the LT-HSC pool in mouse BM, the LT-HSC only rebounded to ~10% of their number in the steady state[86]. However, both the more differentiated HSPC populations as well as mature hematopoietic populations reconstituted to steady state levels after LT-HSC depletion. These data suggest that the majority of the LT-HSC population is dispensable, and that a minimal number of LT-HSC are required to provide long-lasting generation of hematopoietic cells[86]. Therefore, the decreased number of LT-HSC in BCAP$^{-/-}$ mice may reflect a defect in HSC quiescence, but may not impact long-term maintenance of the mature hematopoietic lineages. This is supported by our HSC transplant data, where BCAP-/- LT-HSC did not replenish their compartment as well as their WT counterparts, but produced equal frequencies of the mature hematopoietic populations as WT LT-HSC (Figure 3.4). Therefore, it will be of interest to test the self-renewal ability of BCAP$^{-/-}$ HSC during demand situations, such as in serial HSC transplantations and after 5-FU treatment.

Overall, we have identified a novel function for BCAP as an inhibitor of HSC proliferation in the BM. The reciprocal decreased number of LT-HSC BCAP$^{-/-}$ mice, and increased LT-HSC proliferation in BCAP$^{-/-}$ mice strongly suggest that BCAP functions to maintain either the quiescent state of the LT-HSC pool, or in sustaining the ability of LT-HSC to self-renew. Furthermore, we identified 274 significantly differentially expressed genes in BCAP$^{-/-}$ HSC compared to WT HSC, suggesting that BCAP interacts with several signaling pathways within the HSC compartment. Future work will aim to determine the fitness of BCAP$^{-/-}$ HSC during serial transplantation, as well as identifying the pathway components that BCAP interacts with in order to identify the direct molecular functions of BCAP in the HSC compartment.

## Chapter 3 Tables

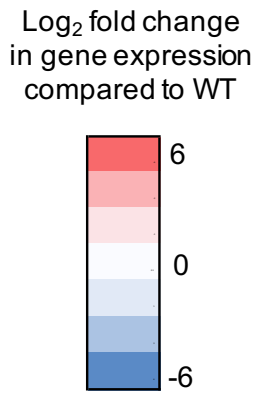


| Gene | logFC | Gene | logFC | Gene | logFC | Gene | logFC | Gene | logFC |
|---|---|---|---|---|---|---|---|---|---|
| Slc1a1 | -5.615349 | Ogt | 0.357619 | Foxp1 | 0.515751 | Egr1 | 0.687812 | Cstf2t | 0.924796 |
| Plscr2 | -3.75403 | Zfp36 | 0.35776 | Lbr | 0.529605 | Stk24 | 0.690703 | Plec | 0.940381 |
| 4430402I18F | -2.984049 | Zfp36l2 | 0.368949 | Rlim | 0.530806 | Tgfbr3 | 0.691812 | Atg4c | 0.953396 |
| Gm4955 | -2.603954 | Hlf | 0.378178 | Hipk1 | 0.530927 | Zfp266 | 0.7009 | Fgfbp3 | 0.965124 |
| Vsig2 | -2.539017 | Set | 0.382089 | Cpsf6 | 0.535064 | Klhl20 | 0.700972 | Trim6 | 0.976006 |
| Prune2 | -1.942666 | Ccnd2 | 0.386114 | Sp1 | 0.536172 | Alyref | 0.700993 | Myof | 0.978425 |
| Ppapdc2 | -1.676817 | Smarce1 | 0.386619 | Slc25a36 | 0.538784 | Map3k1 | 0.704152 | Zbtb10 | 0.978792 |
| Zfp296 | -1.560999 | Crebrf | 0.388951 | Pigm | 0.53902 | Zfp652 | 0.704366 | Marcks | 0.98387 |
| Mfsd2b | -1.426081 | 4833420G17 | 0.390949 | Eya1 | 0.540507 | 2410002F23 | 0.707066 | Etv3 | 0.990854 |
| Hspa1b | -1.360032 | Capns1 | 0.392958 | Tmx4 | 0.541656 | Chchd7 | 0.712474 | Cacfd1 | 0.991979 |
| Ticrr | -1.318415 | Vmp1 | 0.394207 | Socs4 | 0.548354 | Hemk1 | 0.720805 | Kdelc2 | 0.996096 |
| Oas2 | -1.294014 | Taok1 | 0.397028 | Nufip2 | 0.551162 | Fgd4 | 0.728067 | Bend4 | 1.006302 |
| NA | -1.034451 | Coro1c | 0.402166 | Bcl11a | 0.555508 | Vps72 | 0.737129 | Pde4dip | 1.006802 |
| Dcp1a | -1.025599 | Ywhae | 0.405528 | Fstl1 | 0.562656 | Rc3h2 | 0.737375 | Ptp4a1 | 1.016943 |
| Slx4 | -0.906263 | Cdk17 | 0.407375 | Hmgb1 | 0.563377 | 42258 | 0.738232 | Zfhx3 | 1.019129 |
| Cd52 | -0.869186 | Tram1 | 0.409944 | Hcls1 | 0.567999 | Gtf2a1 | 0.73825 | NA | 1.043233 |
| Dhx29 | -0.835879 | Tpm3 | 0.411921 | Nsd1 | 0.571416 | Abi2 | 0.741689 | Pik3ap1 | 1.051362 |
| Tnfaip2 | -0.82717 | Fam208a | 0.414782 | Uty | 0.571912 | 9130023H24 | 0.746863 | Btg1 | 1.063223 |
| Gm20467 | -0.770655 | Fnbp1 | 0.415695 | Ide | 0.576963 | Poldip3 | 0.748311 | Hgs | 1.067731 |
| Ms4a6c | -0.737684 | Malat1 | 0.416856 | Sirpa | 0.577564 | Cbx6 | 0.752975 | Inpp4a | 1.070182 |
| Hsh2d | -0.731279 | Zc3h7a | 0.425745 | Meis1 | 0.584412 | Tmem170b | 0.755389 | NA | 1.075536 |
| Plac8 | -0.689226 | Gimap5 | 0.427413 | Dfna5 | 0.586555 | Wasl | 0.756925 | Cblb | 1.081797 |
| Oas1a | -0.677579 | Foxn3 | 0.438626 | Spin1 | 0.586586 | Znf512b | 0.768221 | Gm15467 | 1.082767 |
| Xaf1 | -0.677563 | Rnf167 | 0.441054 | Cd44 | 0.594835 | Hsdl1 | 0.768714 | Ggt5 | 1.089669 |
| Ifi27 | -0.669297 | Zbtb38 | 0.443164 | 42249 | 0.594838 | 2010012O05 | 0.772353 | Fam53c | 1.090556 |
| Zfp622 | -0.655408 | Med13l | 0.444289 | AW549877 | 0.597621 | Vamp4 | 0.77517 | NA | 1.103045 |
| Luzp1 | -0.587993 | Irf2bp2 | 0.446603 | Junb | 0.604697 | Exoc8 | 0.77845 | Mn1 | 1.11405 |
| Stard4 | -0.579044 | Ywhaz | 0.446897 | Kdsr | 0.606194 | C330006A16 | 0.779183 | Sugct | 1.16595 |
| Asap1 | -0.521456 | Srpk1 | 0.454197 | Rnf44 | 0.608543 | Spcs3 | 0.782648 | Tpt1 | 1.182575 |
| Ly6a | -0.496104 | Pten | 0.457739 | Nucks1 | 0.615732 | Trim23 | 0.784026 | Bcl7a | 1.184595 |
| Tmem40 | -0.495912 | Runx1 | 0.458596 | Larp4b | 0.619502 | Dhrs3 | 0.784875 | Ets1 | 1.19043 |
| Nop56 | -0.480951 | Jun | 0.459759 | Cdc42bpa | 0.631717 | Slc35d1 | 0.786075 | Tspan5 | 1.223421 |
| Ndufs2 | -0.474775 | Tnpo1 | 0.466439 | Zak | 0.631886 | Msi2 | 0.786227 | Gm9958 | 1.231344 |
| Atp6v1a | -0.459412 | Irf2 | 0.46683 | Nrxn1 | 0.631921 | Mysm1 | 0.791004 | Dip2c | 1.247991 |
| Ncapd2 | -0.438992 | Gata2 | 0.468637 | Ganc | 0.635841 | Wrb | 0.794275 | Slc5a3 | 1.280366 |
| Stat1 | -0.437949 | Pafah1b2 | 0.471237 | Ubl3 | 0.638132 | Sfxn3 | 0.797032 | Samd14 | 1.294522 |
| Cops8 | -0.385101 | Krit1 | 0.478513 | Jund | 0.639029 | Ski | 0.811259 | Nck2 | 1.337125 |
| Rapgef6 | -0.381949 | Nipsnap1 | 0.483207 | Tcf7l2 | 0.639307 | Dpysl2 | 0.813428 | Arl3 | 1.341642 |
| Lims1 | -0.272389 | Zfand5 | 0.483728 | Mtx3 | 0.641214 | Tnfrsf26 | 0.819913 | Zfp395 | 1.342877 |
| Bbx | -0.243625 | Srsf5 | 0.484129 | Tmem248 | 0.642836 | Ubfd1 | 0.821188 | Ybey | 1.384436 |
| Prkar1a | 0.226637 | Git2 | 0.484522 | Tug1 | 0.646727 | Dip2b | 0.83245 | NA | 1.402995 |
| Cops6 | 0.242062 | Mecp2 | 0.490243 | Ypel5 | 0.647011 | Ppm1k | 0.840095 | Gm21685 | 1.405615 |
| Sdf4 | 0.26636 | Hiatl1 | 0.490787 | Ccdc6 | 0.647361 | 4930447C04 | 0.842894 | NA | 1.457064 |
| Fam65b | 0.278757 | Ino80d | 0.491982 | Pfas | 0.648963 | Ecscr | 0.843264 | Khsrp | 1.487609 |
| Zfp608 | 0.2819 | Csde1 | 0.494719 | Naa30 | 0.649759 | NA | 0.844632 | Igf1r | 1.542266 |
| Mkln1 | 0.299361 | Clk1 | 0.495524 | Ppp5c | 0.652844 | Mief1 | 0.858339 | Fosb | 1.549126 |
| Mtdh | 0.302243 | Rab31 | 0.499462 | Sec61a1 | 0.655023 | Alg11 | 0.859388 | Kmt2d | 1.551819 |
| Trp53 | 0.315038 | Znrf1 | 0.50015 | Qk | 0.657037 | Braf | 0.866633 | Dvl3 | 1.614423 |
| Canx | 0.320254 | Slc38a2 | 0.50018 | Rfx3 | 0.661149 | Gm9752 | 0.869198 | NA | 1.618157 |
| NA | 0.322659 | Slc2a3 | 0.501784 | Med1 | 0.661396 | BC030336 | 0.873078 | Alpk3 | 1.656754 |
| Mgea5 | 0.325648 | Pan3 | 0.5033 | Mier3 | 0.666354 | Vash1 | 0.880119 | NA | 1.67275 |
| Thrap3 | 0.331101 | Grb10 | 0.504126 | Lrrc58 | 0.670313 | Trio | 0.894267 | Mfsd4 | 2.794268 |
| Apobec3 | 0.342621 | Syncrip | 0.504443 | Ubl7 | 0.673666 | Ptges3 | 0.899288 | Cnr1 | 3.43788 |
| Sp110 | 0.350575 | Gls | 0.512782 | Hk2 | 0.676231 | Arl15 | 0.919016 | Kazald1 | 5.199631 |
| Ikzf2 | 0.352403 | Arglu1 | 0.51565 | Cd274 | 0.679366 | Vldlr | 0.919488 | | |

**Table 3.1 Differentially expressed genes in BCAP$^{-/-}$ HSC.** Table listing the 274 differentially expressed genes in BCAP$^{-/-}$ HSC compared to WT HSC, according to RNA sequencing analysis as shown in Figure 3.3. RNA sequencing conducted on total mRNA isolated from 750 sorted LT-HSC and 750 sorted ST-HSC from steady-state WT and BCAP$^{-/-}$ mice, with n= 4 mice per group. Differentially expressed genes in table were identified as genes showing differences in expression between WT and BCAP$^{-/-}$ HSC with an adjusted p-value < 0.05. Numbers reflect $\log_2$ fold change, with negative values representing increased expression in BCAP$^{-/-}$ HSC, and positive values representing increased expression in WT HSC. Heatmap colorization was used to visualize differences in $\log_2$ fold change, as indicated in legend.

**Chapter 3 Figures**

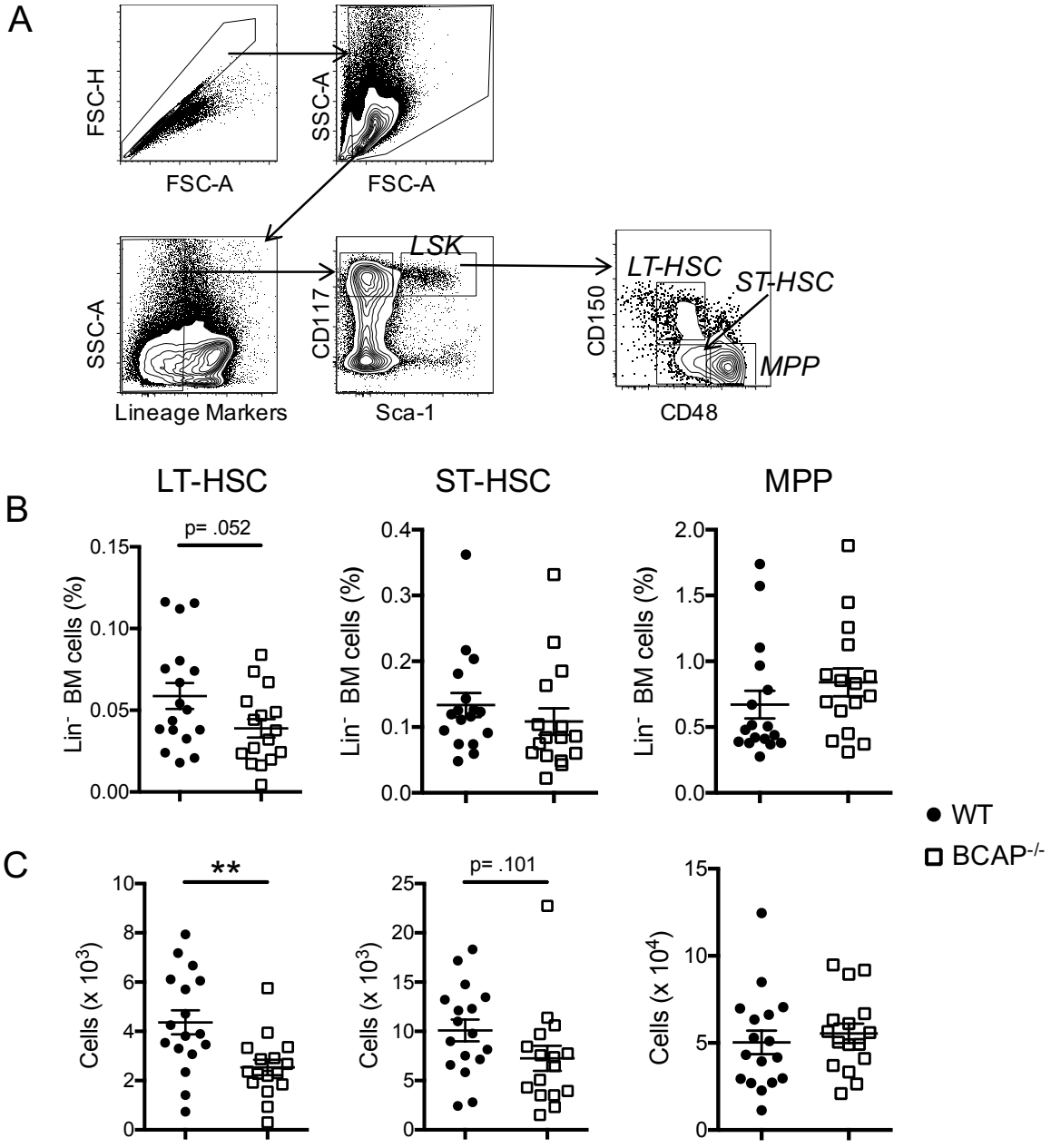


**Figure 3.1. Decreased number of LT-HSC in steady-state BCAP$^{-/-}$ BM.** (A) Identification of HSPC populations from Lineage$^-$ BM of WT mouse by flow cytometry. Cells were identified from live cell gating as follows: LT-HSC (Lin$^-$CD117$^+$Sca1$^+$CD150$^+$CD48$^-$), ST-HSC (Lin$^-$CD117$^+$Sca1$^+$CD150$^-$CD48$^-$), MPP (Lin$^-$CD117$^+$Sca1$^+$CD150$^-$CD48$^+$). (B) Frequency of LT-HSC (left), ST-HSC (middle), and MPP (right) within Lin$^-$ BM of WT and BCAP$^{-/-}$ mice. (C) Absolute numbers of LT-HSC (left), ST-HSC (middle), and MPP (right) in BM of WT and BCAP$^{-/-}$ mice. Data are pooled from 4 independent experiments, with n= 16-17 mice per group. For all graphs, data show mean +/- SEM; each symbol represents data from an individual mouse. * $p< 0.05$, ** $p< 0.01$, as determined by two-tailed, unpaired Student's *t* test.

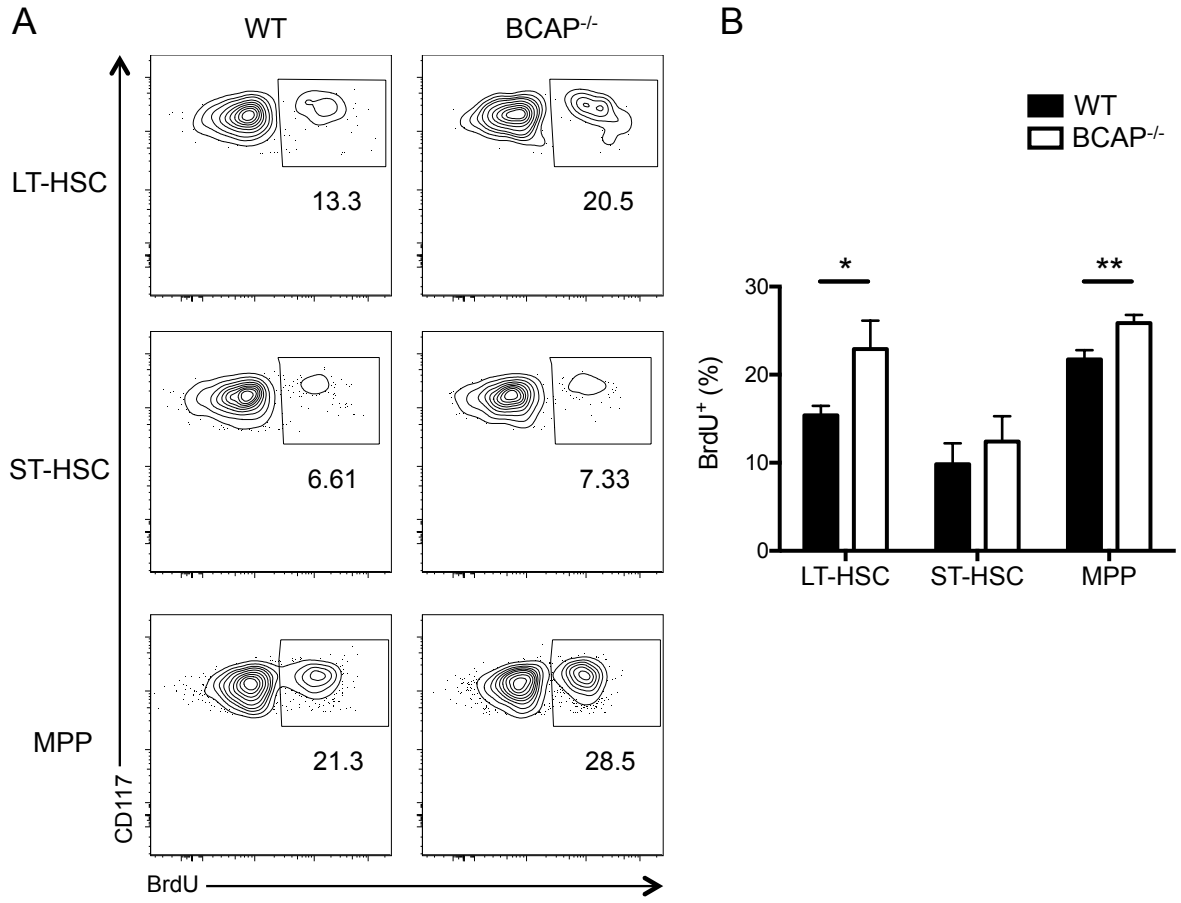


**Figure 3.2. Increased Proliferation in steady-state LT-HSC and MPP in BCAP$^{-/-}$ mice.** (A) Representative flow plots showing BrdU$^{+}$ cells among LT-HSC (top), ST-HSC (middle), and MPP (bottom) from WT and BCAP$^{-/-}$ mice given a 1 hour pulse i.p. with 1 mg BrdU. Numbers represent frequency of BrdU$^{+}$ cells within indicated population. (B) Frequencies of BrdU$^{+}$ LT-HSC, ST-HSC, and MPP from WT and BCAP$^{-/-}$ mice. Data are pooled from 3 independent experiments, with n= 10-11 mice per group. Graph shows mean + SEM; * $p< 0.05$, ** $p< 0.01$, as determined by two-tailed, unpaired Student's *t* test.

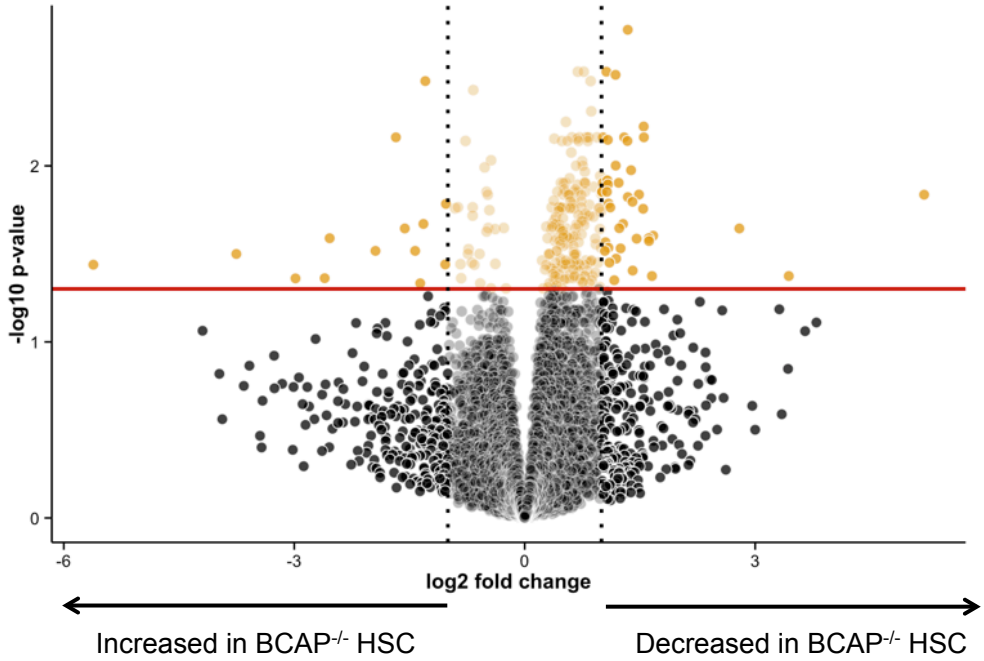


**Figure 3.3. Volcano plot analysis of differentially expressed genes in BCAP$^{-/-}$ HSC.** The differentially expressed genes from RNA sequencing between BCAP$^{-/-}$ and WT HSC displayed as a volcano plot. RNA sequencing conducted on total mRNA isolated from 750 sorted LT-HSC and 750 sorted ST-HSC from steady-state WT and BCAP$^{-/-}$ mice, with n= 4 mice per group. Differential gene expression shown as $\log_2$ fold change comparing WT to BCAP$^{-/-}$ HSC on the x-axis, with adjusted p-value ($-\log_{10}$) shown on the y-axis. Each colored dot represents an individual gene detected by RNA sequencing. Horizontal red line represents demarcation for genes with adjusted p-value $\leq 0.05$. Yellow dots represent genes with adjusted p-value $\leq 0.05$. Dots inside the dashed black lines represent genes with differential expression fold change of $\leq 2$ ($\log_2 FC \leq 1$). In total, 274 genes were differentially expressed in BCAP$^{-/-}$ HSC compared to WT HSC, with 57 genes showing > 2 fold change difference between BCAP$^{-/-}$ and WT HSC.

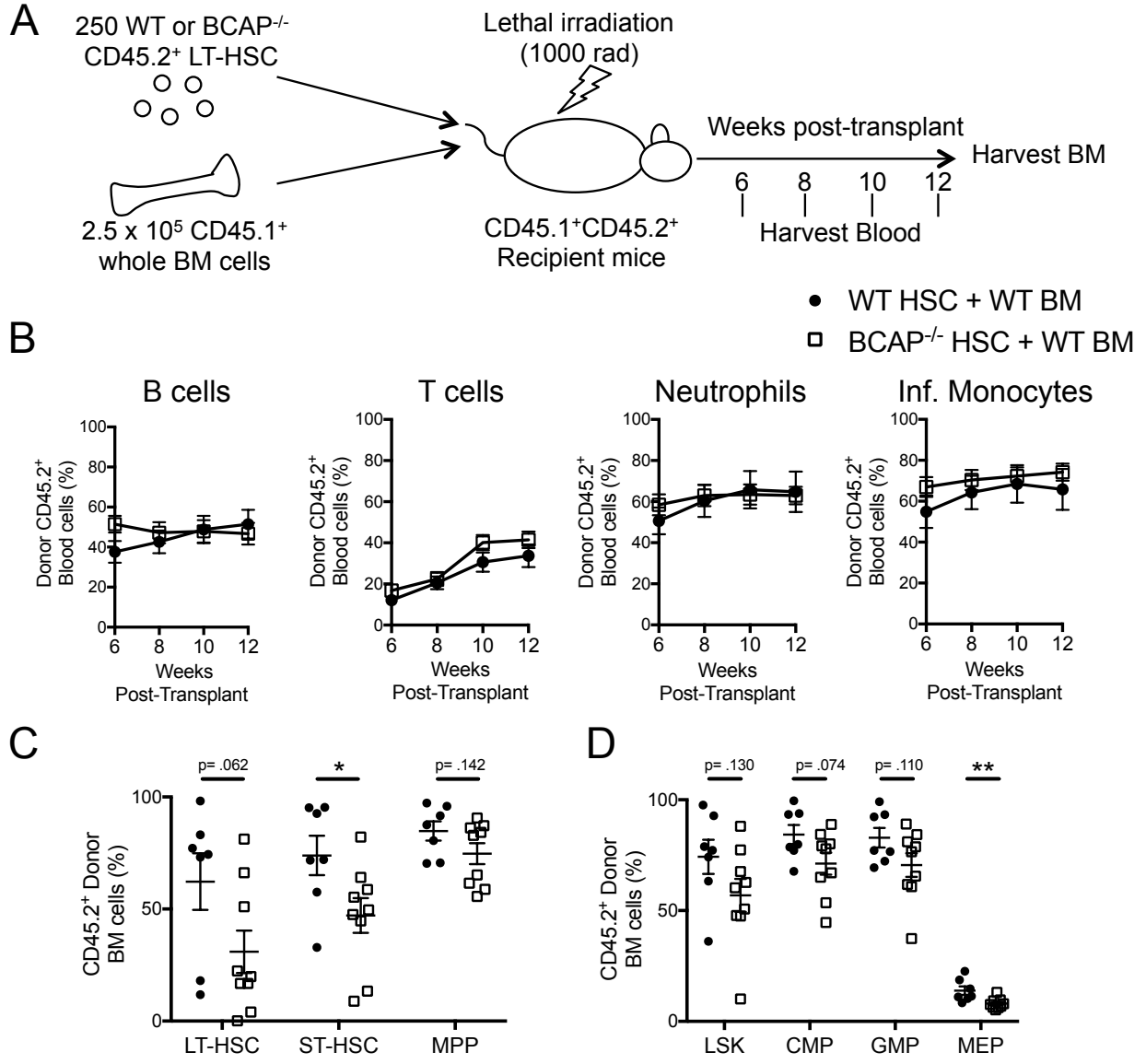


**Figure 3.4. Diminished HSC reconstitution in BCAP$^{-/-}$ primary HSC transplants.** A. Protocol showing production of WT or BCAP$^{-/-}$ HSC transplant mice. B. Frequency of donor-cell-derived (CD45.2$^{+}$) B cells (CD19$^{+}$ cells), T cells (TCRβ$^{+}$ cells), Neutrophils (Ly6G$^{+}$ Ly6C$^{int}$CD11b$^{+}$ cells) and Inflammatory Monocytes (Ly6G$^{-}$Ly6C$^{hi}$CD11b$^{+}$ cells) in the blood of HSC transplant mice at the indicated time points post-transplant. C. Frequency of donor-cell-derived (CD45.2$^{+}$) LT-HSC, ST-HSC, and MPP cells in the BM of HSC transplant mice at 25 weeks post transplantation. D. Frequency of donor-cell-derived (CD45.2$^{+}$) LSK, CMP, GMP, and MEP cells in the BM of HSC transplant mice at 25 weeks post-transplant. Graph shows mean +/- SEM; * $p< 0.05$, ** $p< 0.01$, as determined by two-tailed, unpaired Student's *t* test.

# CHAPTER 4: CONCLUDING REMARKS

Here we have identified several novel functions for BCAP within HSPC. BCAP functions as an inhibitor the proliferation and differentiation of myeloid cells from the HSPC in the steady state and during demand situations[72]. Additionally, BCAP maintains the LT-HSC population size and inhibits proliferation of LT-HSC and MPP, suggesting that BCAP functions as a positive regulator of HSC quiescence and/or self-renewal. Lastly, we identified 274 differentially expressed genes within BCAP$^{-/-}$ HSC, providing greater insight into the role BCAP plays within the various transcriptional and signaling pathways controlling HSC function. Overall, we have identified BCAP as a dynamic regulator of hematopoiesis and myeloid cell differentiation.

BCAP was originally described to activate PI3K by interacting with the p85 subunit of PI3K upon phosphorylation of its four YxxM motifs[38]. However, BCAP contains several additional protein-protein interaction domains, including ankyrin repeats, a DBB domain, coiled-coil domains, proline-rich sequences and a "cryptic-TIR domain[37,38,45]." Thus, BCAP may interact with several signaling pathways in addition to PI3K, and additionally may regulate more than one pathway in HSPC. Interestingly, PI3K signaling has been shown to promote proliferation and differentiation of HSPC, and particularly supports myeloid differentiation[68]. Therefore, the increased proliferation in LT-HSC found in BCAP$^{-/-}$ suggests that BCAP interacts with other pathways to modulate HSC proliferation. Further examination into the proteins directly interacting with BCAP will provide a greater understanding for which signaling pathways critical for HSPC differentiation associate with BCAP.

Over 150 genes have been identified via knockout mouse studies to have a role in hematopoiesis, with phenotypes ranging from mild to severe[70]. Whereas the majority of these

knockout mice had defects in hematopoiesis, only 24 of the studied mouse strains exhibited increased hematopoiesis. These included the E3 ubiquitin protein ligase Cbl[87], the transcription factors Egr1[78] and Hif1α[88], and the dioxygenase Tet2[89]. Many genes whose deficiency results in increased hematopoiesis are also associated with malignancy, such as *Tet2*[90], and with myeloproliferative disorders, such as the combination of *Cbl* and *Cblb*[91]. Here, we show that BCAP$^{-/-}$ mice represent a strain with increased hematopoietic activity, though we have not seen leukemia or myeloproliferative disorders in BCAP$^{-/-}$ mice. Future work will examine whether BCAP deficiency promotes these hematopoietic disorders using leukemia prone mouse models.

Understanding the pathways that control hematopoiesis at the steady state and during demand situations is of great interest, as disruption of this process can result in BM failure and malignancy[1,70,71]. Furthermore, factors that affect HSPC differentiation may lead to clinical interventions, such as supporting HSPC engraftment following BM transplantation, augmenting HSPC myeloid differentiation during infection or drug-induced myeloablation, and repairing HSPC defects that result in hematological malignancy. Additionally, BCAP may function as a positive regulator of LT-HSC numbers, suggesting that BCAP either promotes or inhibits hematopoietic differentiation at different stages. BCAP represents a unique protein that functions in hematopoiesis by inhibiting myeloid differentiation from both early and late hematopoietic progenitors. Further examination of the mechanisms by which BCAP controls HSPC differentiation is of substantial interest, and may lead to new strategies in manipulating HSPC differentiation and survival within clinical settings. Overall, we have identified BCAP as a novel dynamic regulator of hematopoiesis and myeloid cell development from HSPC in both the steady state and during situations of demand.

# REFERENCES


1. Orkin SH, Zon LI. Hematopoiesis: An Evolving Paradigm for Stem Cell Biology. *Cell*. 2008;132(4):631–644.
2. Doulatov S, Notta F, Laurenti E, Dick JE. Hematopoiesis: A Human Perspective. *Cell Stem Cell*. 2012;10(2):120–136.
3. Akashi K, Traver D, Miyamoto T, Weissman IL. A clonogenic common myeloid progenitor that gives rise to all myeloid lineages. *Nature*. 2000;404(6774):193–197.
4. Iwasaki H, Akashi K. Myeloid Lineage Commitment from the Hematopoietic Stem Cell. *Immunity*. 2007;26(6):726–740.
5. Takizawa H, Boettcher S, Manz MG. Demand-adapted regulation of early hematopoiesis in infection and inflammation. *Blood*. 2012;119(13):2991–3002.
6. Zhao JL, Ma C, O'Connell RM, et al. Conversion of Danger Signals into Cytokine Signals by Hematopoietic Stem and Progenitor Cells for Regulation of Stress-Induced Hematopoiesis. *Cell Stem Cell*. 2014;14(4):445–459.
7. Liu A, Wang Y, Ding Y, et al. Cutting Edge: Hematopoietic Stem Cell Expansion and Common Lymphoid Progenitor Depletion Require Hematopoietic-Derived, Cell-Autonomous TLR4 in a Model of Chronic Endotoxin. *J. Immunol.* 2015;195(6):2524–2528.
8. Buechler MB, Akilesh HM, Hamerman JA. Cutting Edge: Direct Sensing of TLR7 Ligands and Type I IFN by the Common Myeloid Progenitor Promotes mTOR/PI3K-Dependent Emergency Myelopoiesis. *J. Immunol.* 2016;197(7):2577–2582.
9. Lieschke GJ, Grail D, Hodgson G, et al. Mice lacking granulocyte colony-stimulating factor have chronic neutropenia, granulocyte and macrophage progenitor cell deficiency, and impaired neutrophil mobilization. *Blood*. 1994;84(6):1737–1746.
10. Boettcher S, Gerosa RC, Radpour R, et al. Endothelial cells translate pathogen signals into G-CSF-driven emergency granulopoiesis. *Blood*. 2014;124(9):1393–1403.
11. Weber GF, Chousterman BG, He S, et al. Interleukin-3 amplifies acute inflammation and is a potential therapeutic target in sepsis. *Science*. 2015;347(6227):1260–1265.
12. Kopf M, Baumann H, Freer G, et al. Impaired immune and acute-phase responses in interleukin-6-deficient mice. *Nature*. 1994;368(6469):339–342.
13. Maeda K, Malykhin A, Teague-Weber BN, et al. Interleukin-6 aborts lymphopoiesis and elevates production of myeloid cells in systemic lupus erythematosus–prone B6.Sle1.Yaa animals. *Blood*. 2009;113(19):4534–4540.
14. Schürch CM, Riether C, Ochsenbein AF. Cytotoxic CD8+ T cells stimulate hematopoietic progenitors by promoting cytokine release from bone marrow mesenchymal stromal cells. *Cell Stem Cell*. 2014;14(4):460–472.
15. de Bruin AM, Voermans C, Nolte MA. Impact of interferon- on hematopoiesis. *Blood*. 2014;124(16):2479–2486.
16. Essers MAG, Offner S, Blanco-Bose WE, et al. IFNα activates dormant haematopoietic stem cells in vivo. *Nature*. 2009;458(7240):904–908.
17. Buechler MB, Teal TH, Elkon KB, Hamerman JA. Cutting edge: Type I IFN drives emergency myelopoiesis and peripheral myeloid expansion during chronic TLR7 signaling. *J. Immunol.* 2013;190(3):886–891.
18. Scott EW, Fisher RC, Olson MC, et al. PU.1 functions in a cell-autonomous manner to

control the differentiation of multipotential lymphoid-myeloid progenitors. *Immunity*. 1997;6(4):437–447.
19. Fisher RC, Scott EW. Role of PU.1 in hematopoiesis. *Stem Cells*. 1998;16(1):25–37.
20. Friedman AD. C/EBPα in normal and malignant myelopoiesis. *Int. J. Hematol.* 2015;101(4):330–341.
21. Yáñez A, Goodridge HS. Interferon regulatory factor 8 and the regulation of neutrophil, monocyte, and dendritic cell production. *Curr Opin Hematol*. 2016;23(1):11–17.
22. Hamilton JA. Colony-stimulating factors in inflammation and autoimmunity. *Nat Rev Immunol*. 2008.
23. Rieger MA, Hoppe PS, Smejkal BM, Eitelhuber AC, Schroeder T. Hematopoietic cytokines can instruct lineage choice. *Science*. 2009;325(5937):217–218.
24. Dai XM. Targeted disruption of the mouse colony-stimulating factor 1 receptor gene results in osteopetrosis, mononuclear phagocyte deficiency, increased primitive progenitor cell frequencies, and reproductive defects. *Blood*. 2002;99(1):111–120.
25. Auffray C, Sieweke MH, Geissmann F. Blood Monocytes: Development, Heterogeneity, and Relationship with Dendritic Cells. *Annu. Rev. Immunol.* 2009;27(1):669–692.
26. Mossadegh-Keller N, Sarrazin S, Kandalla PK, et al. M-CSF instructs myeloid lineage fate in single haematopoietic stem cells. *Nature*. 2013;497(7448):239–243.
27. Wicks IP, Roberts AW. Targeting GM-CSF in inflammatory diseases. *Nature Reviews Rheumatology*. 2015;12(1):37–48.
28. Zhan Y, Lieschke GJ, Grail D, Dunn AR, Cheers C. Essential Roles for Granulocyte-Macrophage Colony-Stimulating Factor (GM-CSF) and G-CSF in the Sustained Hematopoietic Response of Listeria monocytogenes–Infected Mice. *Blood*. 1998;91(3):863–869.
29. Stanley E, Lieschke GJ, Grail D, et al. Granulocyte/macrophage colony-stimulating factor-deficient mice show no major perturbation of hematopoiesis but develop a characteristic pulmonary pathology. *Proc. Natl. Sci. U.S.A.* 1994.
30. Eaves CJ. Hematopoietic stem cells: concepts, definitions, and the new reality. *Blood*. 2015;125(17):2605–2613.
31. Seita J, Weissman IL. Hematopoietic stem cell: self-renewal versus differentiation. *Wiley Interdisciplinary Reviews: Systems Biology and Medicine*. 2010;2(6):640–653.
32. Wilson NK, Foster SD, Wang X, et al. Combinatorial transcriptional control in blood stem/progenitor cells: genome-wide analysis of ten major transcriptional regulators. *Cell Stem Cell*. 2010;7(4):532–544.
33. Christian Kosan MG. Genetic and Epigenetic Mechanisms That Maintain Hematopoietic Stem Cell Function. *Stem Cells International*. 2016;2016:.
34. Lacombe J, Herblot S, Rojas-Sutterlin S, Haman A. Scl regulates the quiescence and the long-term competence of hematopoietic stem cells. *Blood*. 2010.
35. de Pater E, Kaimakis P, Vink CS, et al. Gata2 is required for HSC generation and survival. *J. Exp. Med*. 2013;210(13):2843–2850.
36. Vicente C, Conchillo A, García-Sánchez MA, Odero MD. The role of the GATA2 transcription factor in normal and malignant hematopoiesis. *Crit. Rev. Oncol. Hematol.* 2012;82(1):1–17.
37. Yamazaki T, Takeda K, Gotoh K, et al. Essential immunoregulatory role for BCAP in B cell development and function. *J. Exp. Med.* 2002;195(5):535–545.
38. Okada T, Maeda A, Iwamatsu A, Gotoh K, Kurosaki T. BCAP: the tyrosine kinase

substrate that connects B cell receptor to phosphoinositide 3-kinase activation. *Immunity*. 2000;13(6):817–827.
39. Yamazaki T, Kurosaki T. Contribution of BCAP to maintenance of mature B cells through c-Rel. *Nat. Immunol.* 2003;4(8):780–786.
40. Castello A, Gaya M, Tucholski J, et al. Nck-mediated recruitment of BCAP to the BCR regulates the PI(3)K-Akt pathway in B cells. *Nat. Immunol*. 2013;14(9):966–975.
41. Inabe K, Kurosaki T. Tyrosine phosphorylation of B-cell adaptor for phosphoinositide 3-kinase is required for Akt activation in response to CD19 engagement. *Blood*. 2002;99(2):584–589.
42. Aiba Y, Kameyama M, Yamazaki T, Tedder TF, Kurosaki T. Regulation of B-cell development by BCAP and CD19 through their binding to phosphoinositide 3-kinase. *Blood*. 2007;111(3):1497–1503.
43. MacFarlane AW, Yamazaki T, Fang M, et al. Enhanced NK-cell development and function in BCAP-deficient mice. *Blood*. 2008;112(1):131–140.
44. Ni M, MacFarlane AW, Toft M, et al. B-cell adaptor for PI3K (BCAP) negatively regulates Toll-like receptor signaling through activation of PI3K. *Proc. Natl. Acad. Sci. U.S.A.* 2012;109(1):267–272.
45. Troutman TD, Hu W, Fulenchek S, et al. Role for B-cell adapter for PI3K (BCAP) as a signaling adapter linking Toll-like receptors (TLRs) to serine/threonine kinases PI3K/Akt. *Proc. Natl. Acad. Sci. U.S.A.* 2012;109(1):273–278.
46. Hohl TM, Rivera A, Lipuma L, et al. Inflammatory Monocytes Facilitate Adaptive CD4 T Cell Responses during Respiratory Fungal Infection. *Cell Host & Microbe*. 2009;6(5):470–481.
47. Buechler MB, Gessay GM, Srivastava S, Campbell DJ, Hamerman JA. Hematopoietic and nonhematopoietic cells promote Type I interferon- and TLR7-dependent monocytosis during low-dose LCMV infection. *Eur. J. Immunol.* 2015;45(11):3064–3072.
48. Rosenbauer F, Tenen DG. Transcription factors in myeloid development: balancing differentiation with transformation. *Nat Rev Immunol*. 2007;7(2):105–117.
49. Yáñez A, Ng MY, Hassanzadeh-Kiabi N, Goodridge HS. IRF8 acts in lineage-committed rather than oligopotent progenitors to control neutrophil vs monocyte production. *Blood*. 2015;125(9):1452–1459.
50. Bernad A, Kopf M, Kulbacki R, et al. Interleukin-6 is required in vivo for the regulation of stem cells and committed progenitors of the hematopoietic system. *Immunity*. 1994;1(9):725–731.
51. Nakamura K, Kouro T, Kincade PW, et al. Src Homology 2–containing 5-Inositol Phosphatase (SHIP) Suppresses an Early Stage of Lymphoid Cell Development through Elevated Interleukin-6 Production by Myeloid Cells in Bone Marrow. *J. Exp. Med.* 2004;199(2):243–254.
52. Reynaud D, Pietras E, Barry-Holson K, et al. IL-6 controls leukemic multipotent progenitor cell fate and contributes to chronic myelogenous leukemia development. *Cancer Cell*. 2011;20(5):661–673.
53. Maeda K, Baba Y, Nagai Y, et al. IL-6 blocks a discrete early step in lymphopoiesis. *Blood*. 2005;106(3):879–885.
54. Walker F, Zhang HH, Matthews V, et al. IL6/sIL6R complex contributes to emergency granulopoietic responses in G-CSF- and GM-CSF-deficient mice. *Blood*. 2008;111(8):3978–3985.

55. Serbina NV, Pamer EG. Monocyte emigration from bone marrow during bacterial infection requires signals mediated by chemokine receptor CCR2. *Nat. Immunol.* 2006;7(3):311–317.
56. Jacquelin S, Licata F, Dorgham K, et al. CX3CR1 reduces Ly6Chigh-monocyte motility within and release from the bone marrow after chemotherapy in mice. *Blood*. 2013;122(5):674–683.
57. Park SI, Liao J, Berry JE, et al. Cyclophosphamide creates a receptive microenvironment for prostate cancer skeletal metastasis. *Cancer Res.* 2012;72(10):2522–2532.
58. Serbina NV, Salazar-Mather TP, Biron CA, Kuziel WA, Pamer EG. TNF/iNOS-producing dendritic cells mediate innate immune defense against bacterial infection. *Immunity*. 2003;19(1):59–70.
59. Shi CC, Hohl TMT, Leiner II, et al. Ly6G+ neutrophils are dispensable for defense against systemic Listeria monocytogenes infection. *J. Immunol.* 2011;187(10):5293–5298.
60. Shi C, Velázquez P, Hohl TM, et al. Monocyte trafficking to hepatic sites of bacterial infection is chemokine independent and directed by focal intercellular adhesion molecule-1 expression. *J. Immunol.* 2010;184(11):6266–6274.
61. Serbina NV, Hohl TM, Cherny M, Pamer EG. Selective expansion of the monocytic lineage directed by bacterial infection. *J. Immunol.* 2009;183(3):1900–1910.
62. Khosravi A, Yáñez A, Price JG, et al. Gut microbiota promote hematopoiesis to control bacterial infection. *Cell Host & Microbe*. 2014;15(3):374–381.
63. Ogawa M. Differentiation and proliferation of hematopoietic stem cells. *Blood*. 1993;81(11):2844–2853.
64. Huber R, Pietsch D, Günther J, et al. Regulation of monocyte differentiation by specific signaling modules and associated transcription factor networks. *Cell. Mol. Life Sci.* 2013;71(1):63–92.
65. Romani L, Mencacci A, Cenci E, et al. Impaired neutrophil response and CD4+ T helper cell 1 development in interleukin 6-deficient mice infected with Candida albicans. *J. Exp. Med.* 1996;183(4):1345–1355.
66. Nishii H, Nomura M, Fujimoto N, Matsumoto T. Up-regulation of interleukin-6 gene expression in cyclophosphamide-induced cystitis in mice: An in situ hybridization histochemical study. *Int. J. Urol.* 2006;13(10):1339–1343.
67. Hettinger J, Richards DM, Hansson J, et al. Origin of monocytes and macrophages in a committed progenitor. *Nat. Immunol*. 2013;14(8):821–830.
68. Buitenhuis M, Coffer PJ. The role of the PI3K-PKB signaling module in regulation of hematopoiesis. *Cell Cycle*. 2009;8(4):560–566.
69. Boettcher S, Manz MG. Sensing and translation of pathogen signals into demand-adapted myelopoiesis. *Curr Opin Hematol*. 2016;23(1):5–10.
70. Rossi L, Lin KK, Boles NC, et al. Less is more: unveiling the functional core of hematopoietic stem cells through knockout mice. *Cell Stem Cell*. 2012;11(3):302–317.
71. Vainchenker W, Kralovics R. Genetic basis and molecular pathophysiology of classical myeloproliferative neoplasms. *Blood*. 2017;129(6):667–679.
72. Duggan JM, Buechler MB, Olson RM, Hohl TM, Hamerman JA. BCAP inhibits proliferation and differentiation of myeloid progenitors in the steady state and during demand situations. *Blood*. 2017. 10.1182/blood-2016-06-719823.
73. Sato T, Onai N, Yoshihara H, et al. Interferon regulatory factor-2 protects quiescent hematopoietic stem cells from type I interferon-dependent exhaustion. *Nature Medicine*.

2009;15(6):696–700.
74. Challen GA, Sun D, Jeong M, et al. Dnmt3a is essential for hematopoietic stem cell differentiation. *Nat. Genet.* 2012;44(1):23–31.
75. Challen GA, Sun D, Mayle A, et al. Dnmt3a and Dnmt3b have overlapping and distinct functions in hematopoietic stem cells. *Cell Stem Cell*. 2014;15(3):350–364.
76. Ichikawa M, Goyama S, Asai T, et al. AML1/Runx1 Negatively Regulates Quiescent Hematopoietic Stem Cells in Adult Hematopoiesis. *J. Immunol.* 2008;180(7):4402–4408.
77. Gilmour J, Assi SA, Jaegle U, et al. A crucial role for the ubiquitously expressed transcription factor Sp1 at early stages of hematopoietic specification. *Development*. 2014;141(12):2391–2401.
78. Min IM, Pietramaggiori G, Kim FS, et al. The transcription factor EGR1 controls both the proliferation and localization of hematopoietic stem cells. *Cell Stem Cell*. 2008;2(4):380–391.
79. Luis TC, Naber BAE, Roozen PPC, et al. Canonical wnt signaling regulates hematopoiesis in a dosage-dependent fashion. *Cell Stem Cell*. 2011;9(4):345–356.
80. Huang J, Nguyen-McCarty M, Hexner EO, Danet-Desnoyers G, Klein PS. Maintenance of hematopoietic stem cells through regulation of Wnt and mTOR pathways. *Nature Medicine*. 2012;18(12):1778–1785.
81. Geest CR, Coffer PJ. MAPK signaling pathways in the regulation of hematopoiesis. *J. Leuk. Bio.* 2009;86(2):237-250.
82. Xia P, Wang S, Du Y, et al. Insulin-InsR signaling drives multipotent progenitor differentiation toward lymphoid lineages. *J. Exp. Med.* 2015;212(13):2305–2321.
83. Chian R, Young S, Danilkovitch-Miagkova A, et al. Phosphatidylinositol 3 kinase contributes to the transformation of hematopoietic cells by the D816V c-Kit mutant. *Blood*. 2001;98(5):1365–1373.
84. Green BD, Jabbour AM, Sandow JJ, et al. Akt1 is the principal Akt isoform regulating apoptosis in limiting cytokine concentrations. *Cell Death Differ*. 2013;20(10):1341–1349.
85. Juntilla MM, Patil VD, Calamito M, et al. AKT1 and AKT2 maintain hematopoietic stem cell function by regulating reactive oxygen species. *Blood*. 2010;115(20):4030–4038.
86. Schoedel KB, Morcos MNF, Zerjatke T, et al. The bulk of the hematopoietic stem cell population is dispensable for murine steady-state and stress hematopoiesis. *Blood*. 2016;128(19):2285–2296.
87. Rathinam C, Thien CBF, Langdon WY, Gu H, Flavell RA. The E3 ubiquitin ligase c-Cbl restricts development and functions of hematopoietic stem cells. *Genes Dev.* 2008;22(8):992–997.
88. Takubo K, Goda N, Yamada W, et al. Regulation of the HIF-1alpha level is essential for hematopoietic stem cells. *Cell Stem Cell*. 2010;7(3):391–402.
89. Ko M, Bandukwala HS, An J, et al. Ten-Eleven-Translocation 2 (TET2) negatively regulates homeostasis and differentiation of hematopoietic stem cells in mice. *Proc. Natl. Acad. Sci. U.S.A.* 2011;108(35):14566–14571.
90. Nakajima H, Kunimoto H. TET2 as an epigenetic master regulator for normal and malignant hematopoiesis. *Cancer Sci.* 2014;105(9):1093–1099.
91. Mayumi Naramura NNHGVBHB. Rapidly fatal myeloproliferative disorders in mice with deletion of Casitas B-cell lymphoma (Cbl) and Cbl-b in hematopoietic stem cells. *Proc. Natl. Acad. Sci. U.S.A.* 2010;107(37):16274–16279.

# CURRICULUM VITA


## Jeffrey M. Duggan

E-mail: jmduggan@uw.edu
Phone: (281)435-9331


**Education**

**University of Washington**, Seattle, WA *Anticipated Graduation: March 2017*
Degree: Doctor of Philosophy Candidate, Immunology
Cumulative GPA: 3.73/4.0

**Texas A&M University**, College Station, TX *Graduated: May 2008*
Degree: Bachelor of Science, Biology
Cumulative GPA: 3.67/4.0

**Research Experience**

**Graduate Dissertation Research in Immunology, Univ. of Washington (2010-Present)**
"The role of B-cell adaptor for PI3-kinase (BCAP) in myeloid cell function, homeostasis and development"
Advisor: Dr. Jessica Hamerman

**Research Assistant, Dept. of Pulmonary Medicine, MD Anderson Cancer Center (2008-2010)**
"Determining Toll-like Receptor synergy in stimulated lung innate resistance against bacterial pneumonia"
Advisor: Dr. Scott Evans

**Undergraduate Research Assistant, Dept. of Biochemistry, Texas A&M University (2007)**
"The role of the S107 holin protein of bacteriophage lambda"
Advisor: Rebecca White (graduate student) and Dr. Ry Young

**Undergraduate Research Assistant, Dept. of Biology, Texas A&M University (2007)**
"Examining the correlation between ciliary row configuration and swimming patterns in Paramecium tetraurelia"
Advisor: Dr. Karl Aufderheide

**Honors and Awards**

2016 UW Immunology Sandra L. Clark Immunology Education Fund Scientific Travel Award, for ICI 2016, Melbourne, AUS
2016 AAI Travel Grant for ICI 2016, Melbourne, AUS
2016 AAI Trainee Abstract Award, AAI Immunology 2016, Seattle, WA
2015 AAI Trainee Abstract Award, AAI Immunology 2015, New Orleans, LA
2015 AAI Laboratory Travel Grant, AAI Immunology 2015, New Orleans, LA
2015 Best Poster Award- Graduate Student, UW Immunology 26th Annual Retreat, Seattle, WA
2015 Ray Owen Young Investigator Award for Outstanding Presentation- Graduate Student, 54th Midwinter Conference of Immunologists, Pacific Grove, CA
2014-2015 T32 AI106677 NIAID Training Grant administered by UW Immunology

2011-
2013 T32 CA009537 NCI Training Grant administered by UW Immunology
2010 Division of Internal Medicine Performance Award, MD Anderson Cancer Center, Houston, TX
2009 ATS-Bayer Pharmaceuticals Travel Award, ATS International, San Diego, CA
2008 Graduation Honors: *cum laude*, Texas A&M University, College Station, TX
2008 Dept. of Biology Distinguished Graduate Award, Texas A&M University, College Station, TX
2006 Distinguished Student Award and Tuition Scholarship, Texas A&M University, College Station, TX

**Publications**

Carpentier SJ, Ni M, **Duggan JM**, James RG, Cookson BT, Hamerman JA. (2017) BCAP inhibits inflammasome activation through interaction with Flightless1. *In Preparation*.

Kanter JE, Kramer F, Barnhart S, **Duggan JM**, Chait A, Bouman SD, Hamerman JA, Hansen BF, Olsen GS, Bornfeldt KE. (2017) A glucose-lowering peptide with marked anti-atherosclerotic effects generated through insulin mimicry. *Under Review. Nat. Medicine.*

**Duggan JM**, Buechler, MB, Olson RM, Hohl TM, Hamerman JA. (2017) BCAP inhibits proliferation and differentiation of myeloid progenitors in the steady state and during demand situations. *Blood*. doi:10.1182/blood-2016-06-719823. Epub 2017 Jan 13.

**Duggan JM**, You D, Cleaver JO, Larson DT, Garza RJ, Guzman Pruneda FA, Tuvim MJ, Dickey BF, Evans SE. (2011) Synergistic interactions of TLR2/6 and TLR9 induce a high level of resistance to lung infection in mice. *J. Immunol.* **186,** 5916–5926.

**Presentations**

**Duggan JM,** Buechler MB, Olson RM, Hohl TM, Hamerman JA. 2016. BCAP inhibits myeloid cell development from hematopoietic progenitors. Abstract for oral presentation, ICI 2016, Melbourne, Australia.

**Duggan JM,** Olson RM, Hohl TM**,** Hamerman JA. 2016. BCAP inhibits myeloid cell development from hematopoietic progenitors. Abstract for oral presentation, AAI Immunology 2016, Seattle, WA.

**Duggan JM,** Gessay GM, Krishnamurty A, Hamerman, JA. 2015. BCAP is a negative regulator of myeloid cell development. Abstract for oral presentation, AAI Immunology 2015, New Orleans, LA.

**Duggan JM,** Gessay GM, Krishnamurty A, Hohl TM, Hamerman, JA. 2015. BCAP is a negative regulator of myeloid cell development. Abstract for oral presentation, Midwinter Conference of Immunologists, Pacific Grove, CA.

**Duggan JM**, Krishnamurty A, Gessay GM, Hamerman JA. 2014. The role of BCAP in regulating $CCR2^{+}$ monocyte homeostasis and development. Abstract for oral presentation, UW Immunology $25^{th}$ Annual Retreat, Seattle, WA.

**Duggan JM**, Krishnamurty A, Gessay GM, Hamerman JA. 2013. BCAP regulates innate immunity during *Listeria monocytogenes* infection. Abstract for poster presentation, Midwinter Conference of Immunologists, Pacific Grove, CA.

**Duggan JM**, Hamerman JA. 2012. Dap12 regulates PRR-mediated inflammatory functions of myeloid cells during *Listeria monocytogenes* infection. Abstract for poster presentation, Midwinter Conference of Immunologists, Pacific Grove, CA.

**Duggan JM**, Larson DT, Tuvim MJ, Gilbert B, Dickey, BF, Evans SE. 2009. Toll-like receptor synergy in stimulated innate resistance. Abstract for oral presentation, American Thoracic Society International Conference, San Diego, CA.

## Mentoring/Teaching

**Laboratory Mentor to Rotation Students and Volunteer**, University of Washington (2012-present)
Directed and supervised the research of two rotation students and one participant of the AAI High School Teachers Program

**TA for Undergraduate Immunology Course**, University of Washington (2011)
Instructed students during weekly quiz section
Wrote questions for mid-term exams

## Memberships and Activities

American Association of Immunologists, Trainee Member (2015-2016)
Dept. of Immunology Retreat Planning Committee, Student Member (2010, 2014, & 2015)
Graduate and Professional Student Senate, Senator for Dept. of Immunology, (2010-2011)
American Thoracic Society, Member (2009-2010)